



# Optimization toolbox for Public Bus Transit Electrification

**Technical Report R4**  
**Submitted to IESO Conservation Fund**

**March 2020**

---

**Smart Grid Research Lab**  
**Department of Electrical Engineering &  
Computer Science**  
**Lassonde School of Engineering**  
**YORK UNIVERSITY**



---

# EXECUTIVE SUMMARY

Motivated by the critical need to reduce greenhouse gas (GHG) emissions produced by the transportation sector in Ontario, this project aims to investigate the impact of replacing 100% of existing public transit buses with electric battery-based buses (BEBs), *while continuing to maintain a wide range of transit demand services at an acceptable quality of service*. As a result, an engineering toolbox has been developed to help quantify the economic, operational, and environmental impacts of electrifying public transit buses for different utility and transit service territories within Ontario. The toolbox enables the design, modeling, simulation, and optimization of a fleet of BEBs that consider two main charging options: overnight charging and opportunity (on-route) charging. The toolbox has been used to conduct a set of extended simulations that have resulted in the establishment of an acceptable range for bus charger sizes, as well as overall charging profiles based on their bus route. Broadly, simulations have been executed on transit networks for Mississauga, Brampton, and York Region, in addition to the utility service territory of Alectra Utilities (in the York Region).

The following list summarizes a critical list of observations and conclusions that are drawn from the aforementioned simulations, all of which have operational, economic, and environmental impacts.

1. In totality, Ontario's bulk power system will be expected to serve an additional **1700 GWh/year** of electrical demand due to the electrification of all school, city, and GO buses.
2. A study of a feeder within the Alectra-controlled grid in Vaughan reveals that the peak demand of the feeder will increase from 14MW (without BEBs) to 16.6MW when connecting seven 600 kW chargers along the feeder. This is a peak demand increase of 17%. The voltage of the feeder remains within +/- 5% of the nominal voltage level despite the rise in peak demand.
3. An example study of the Buttonville substation in the Alectra-controlled grid in Markham indicates that the substation capacity (170 MVA) is adequate to service the rise in peak demand caused by bus electrification in the area. The current peak demand of the substation is 130 MW, which rises to approximately 144 MW if 600 kW chargers are added to the system.
4. BEBs that utilize opportunity charging generate high levels of intermittency in electrical demand. A fast-response energy storage system is a suitable technology to smoothen the intermittency and maintain the overall level of power quality within the power system.
5. An operational cost analysis comparing the operating cost (OPEX) of existing diesel buses (fuel costs) to BEBs (charging costs) for the Mississauga, York Region, and Brampton transit networks indicates that BEBs provide OPEX reductions of 50%, while providing maintenance cost reductions of 40%. This translates to annual savings of \$5.69M, \$3.6M, and \$4.82M for Brampton, Mississauga, and York Region, respectively.
6. For the same transit networks referenced in [6], capital expenditure (CAPEX) requirements for BEBs are more than two times higher than diesel buses. Considering the annualized CAPEX and OPEX, BEB deployment adds an additional \$7.89M (32.7% increase), \$10.0M (51% increase), and \$7.16M (36.3% increase) for Mississauga, York Region, and Brampton transit operators, respectively.
7. An environmental impact assessment estimates a 41% reduction of total GHG emissions in Ontario if the BEBs are charged with a standard, non-renewable, electricity supply mix, resulting in the reduction of 430,658 tonnes of carbon dioxide equivalent emissions (tCo<sub>2</sub>-eq.). If the BEBs are charged with 100%

---

renewable energy sources, the corresponding numbers are a 98.4% total reduction of GHG emissions, with savings of 1,031,178 tCO<sub>2</sub>-eq. All metrics are in comparison to using diesel buses.

Broadly, the project concludes that while transit electrification is a necessary and viable step to reduce GHG emissions, further development and enhancements in BEB technology are required to reduce the large CAPEX to deploy the BEBs and for it to be ultimately cost competitive to diesel-based buses. Furthermore, there is a requirement to optimally configure BEB fleets such that their deployment does not violate the existing constraints of both transit and power systems. This project has developed tools for that very purpose, enabling transit/power system operators to design, model, and simulate the impacts of BEB fleets on their networks. The toolbox was tested within this project for several transit networks within the service areas of Alectra Inc., where BEB fleets were optimally designed to obey the physical constraints of the power distribution system **without needing any modification to the existing bus scheduling/timetable.**

The project was conceptualized and managed by Dr. Hany Farag, Associate Professor and York Research Chair. Funded by the Independent Electricity System Operator (IESO) under the IESO Conservation Fund program, the project has been completed in collaboration with Alectra Utilities. The project research team at York University acknowledges the collaboration with Dr. Moataz Mohamed, Assistant Professor in the Civil Engineering Department at McMaster University. Dr. Mohamed is an expert in Transportation Planning and Operation of Transit Systems, and he worked with the research team in the development of the engineering tools for the studies. Also, the research team acknowledges the support letter provided by the Canadian Urban Transit Research & Innovation Consortium (CUTRIC). This project has resulted in the training of several highly qualified personnel (HQP) in the province of Ontario, including postdoctoral research fellows, graduate students, and undergraduate students.

---

## PROJECT TEAM

*Dr. Hany Farag*  
*Associate Professor*

Dr. Farag received the B.Sc. (with honors) and the M.Sc. degrees in Electrical Engineering from Assiut University, Assiut, Egypt, in 2004 and 2007, respectively, and the Ph.D degree in Electrical and Computer Engineering from University of Waterloo, in 2013. Since July 2013, he has been with the Department of Electrical Engineering and Computer Science, Lassonde School of Engineering, York University, where he is currently an Associate Professor. Dr. Farag is a York Research chair in Integrated Smart Energy Grids, the principal investigator of the smart grid research laboratory (SGRL), and the lead developer for the power system curriculum at YorkU, where he has generated over \$2M for lab equipment. Dr. Farag is a registered professional engineer in Ontario and a member of Cigre international workgroup C6.28 for standardization of off-supply microgrids. Dr. Farag is a recipient of the prestigious Early Research Award (ERA) from Ontario Government. His main research interests are in the areas of power systems, integration of distributed and renewable energy resources in smart grids, electrification of transport systems, and applications of multi-agent technologies.

*Nader El-Taweel*  
*PhD Candidate*

Nader El-Taweel received the B.Sc. degree in electrical engineering from Alexandria University, Egypt, in 2013 and the M.A.Sc. degree in electrical engineering from the Lassonde School of Engineering, York University, ON, Canada, in 2016, where he is currently pursuing the Ph.D. degree with the Department of Electrical Engineering and Computer Science. He has received several federal and provincial prestigious awards in Canada, including the Natural Sciences and Engineering Research Council (NSERC) of Canada Postgraduate-Doctoral Scholarship and the Ontario Government Scholarship. In 2018, he has received the Rob Maclsaac Fellowship and joined Metrolinx, a regional transportation agency of the Government of Ontario, to investigate the planning and operation of an electrified GO Bus transit system. His current research focuses on examining solutions to facilitate the adoption of zero-emission transportation fleets. This includes both battery and hydrogen-based technologies of public transit buses and passenger vehicles.

*Abdullah Sawas*  
*PhD Candidate*

Abdullah Sawas is a Ph.D. candidate in the Electrical Engineering and Computer Science (EECS) at York University, Toronto, Canada. His research interests include data analysis, cyber physical security, and smart grids. He holds a M.Sc. in Computing and Information Science from Masdar Institute, Abu Dhabi, United Arab Emirates, and a B.Sc. in Informatics Engineering from the Aleppo University, Aleppo, Syria. Before joining York University, he worked as automation and project engineer in the department of Electrical Engineering and Power System at Saudi Aramco, Dhahran, KSA.

*Gouri Barai*  
*PhD Candidate*

Gouri Barai is a PhD student at the Smart Grid Research Lab. Gouri holds a MASc degree in Electrical & Computer Engineering from Ryerson University, Toronto. She completed her BSc degree in Electrical & Electronic Engineering. She has research experience in energy storage system, smart grid, smart metering and quantum cryptography. Besides the academic career, she is a professional level baker with deep passion for reading and collecting books.

---

# TABLE OF CONTENTS

<b>1. Milestone Deliverables .....</b>	<b>11</b>
<b>2. Utility-Transit Mathematical Model Formulation.....</b>	<b>12</b>
2.1 Modeling of Utility-Transit Toolbox .....	13
2.2 Utility-Transit Model Coding and testing .....	19
2.3 Numerical Results .....	19
2.3.1 Impact on Alectra Feeders .....	19
2.3.1.1 Impact of BEBs on Feeder Loading.....	20
2.3.1.2 Impact of BEBs on Voltage Profile.....	24
2.3.1.3 Impact of BEBs on Substation Capacity.....	25
2.3.1.4 Energy storage for power intermittency minimization .....	27
2.3.2 Case Study for Belleville Transit Electrification.....	28
2.3.2.1 Optimal BEBs configuration .....	31
2.3.2.2 Sensitivity Analysis of the BEBs Configurations.....	33
<b>3. Multi-Regression Model Analysis.....</b>	<b>35</b>
3.1 Introduction .....	35
3.2 Regression Analysis Methods.....	35
3.3 Data Description.....	36
3.4 Regression Model Selection .....	38
3.5 Case Study 1: One Network with all Input Parameters.....	39
3.6 Case Study 2: Accuracy Enhancement .....	40
3.7 Case Study 3: Study with all networks to be trained.....	41
<b>4. Economic Cost and Environmental Impact Assessment.....</b>	<b>43</b>
4.1 Economical Analysis .....	43
4.2 Environmental Analysis.....	45
4.3 Province Level Economic and Environmental Analysis.....	46

---

<b>5. Development of GUI Interface .....</b>	<b>48</b>
5.1 Data Entry and Inspection Interfaces .....	48
5.2 Electric Power Utility and Optimization Setup Interfaces .....	52
5.3 Economic and Environmental Analysis Interfaces.....	55
<b>6. CONCLUSIONS.....</b>	<b>57</b>
<b>7. REFERENCES.....</b>	<b>59</b>

---

## LIST OF FIGURES

Figure 1.1 Framework of the proposed Transit Electrification Toolbox.....	11
Figure 2.1 Framework for the proposed utility–transit optimization model. ....	13
Figure 2.2 Schematic diagram for the transit schedule assignments for a bus b.....	14
Figure 2.3 Schematic diagram for the BEB charging opportunity after each trip j.....	16
Figure 2.4 Calculated One-minute Resolution of Demand Profiles for Different Size Chargers Connected to Feeder 12M3: (a) 300 kW, (b) 450 kW, and (c) 600 kW Chargers. .....	21
Figure 2.5 Feeder 12M3 Hourly Historical Demand Profile .....	21
Figure 2.6: Hourly peak demand for three different charger ratings to be connected to Feeder 12M3.....	22
Figure 2.7: Hourly average demand for three different charger ratings to be connected to Feeder 12M3 .....	22
Figure 2.8: Expected hourly peak demand increase in Feeder 12M3 with three different charger ratings .....	23
Figure 2.9: Expected hourly peak demand percent increase in Feeder 12M3 with three different charger ratings .....	23
Figure 2.10: Expected hourly average demand increase in Feeder 12M3 with three different charger ratings .....	24
Figure 2.11: Expected hourly average demand percent increase in Feeder 12M3 with three different charger ratings .....	24
Figure 2.12: Hourly Feeder 12M3 Minimum Voltage with and without Chargers .....	25
Figure 2.13: Buttonville substation feeders historical demand .....	26
Figure 2.13 YRT transit network charging profile using 300 kW charger and ESS for profile smoothing: (a) charging profile, (b) ESS operation, and (c) ESS state of energy .....	27
Figure 2.14 YRT transit network ESS for profile smoothing: (a) consumption, and (b) State of charge. ....	28
Figure 2.15 Belleville city bus transit map, BEBs assignments data, and its integration with the 33-power distribution system.....	29
Figure 2.16 Typical daily load profile for the studied system.....	29
Figure 2.17 Scenario 2: (a) Speed profile, (b) gradient, and (c) elevation, for Loyalist route. ....	30

Figure 2.18 BEB #9 operated at Loyalist route (a) scenario 2 energy consumption, and (b) scenario 1 and scenario 2 SOC. ....	31
Figure 2.19 The BEBs charging profile at; (a) Scenario 1, and (b) Scenario 2. ....	32
Figure 2.20 The PDS-wide minimum voltage profile for the studied scenarios. ....	33
Figure 2.21 Feasible BEBs configurations at different number of chargers for; (a) Scenario 1, and (b) Scenario 2. ....	34
<i>Figure 3.1 Single versus Multi-Regression analysis models</i> .....	36
Figure 3.1: The correlation between the predictors and the target value (battery size) .....	38
Figure 3.2: Regressor training process .....	38
Figure 3.3: Making prediction using a trained regression model.....	39
Figure 3.4: Predicted versus actual battery size.....	39
Figure 3.5: Sample of the predicted battery size for individual routes of Mississauga Transit Network .....	40
Figure 3.6: Regressor training with preprocessing of the features .....	40
Figure 3.7: Predicted versus actual battery size (using the improved regression model) .....	41
Figure 3.8: Predicted battery size for individual routes of Mississauga Transit Network using improved regression model.....	41
Figure 3.9: The regression errors of the model developed using Mississauga data only .....	42
Figure 4.1 YRT Weekdays vs weekends Operation expenditure (OPEX) .....	44
Figure 4.2 Annualized BEBs vs DB Economic Analysis.....	44
Figure 4.3 BEBs vs DB Environmental Impact .....	46
Figure 5.1 The main screen to enter electric bus specifications .....	49
Figure 5.2 Visualize bus routes and query information about the route .....	49
Figure 5.3 Elevation profile of bus route shown per the distance .....	50
Figure 5.4 A screenshot of block details table .....	50
Figure 5.5 A snapshot of the speed profile generation in the WEBST toolbox .....	51
Figure 5.6 A screenshot of energy consumption analysis output .....	51
Figure 5.7 WEBST interface for entering electric power distribution nodes data.....	52
Figure 5.8 WEBST interface for entering electric power distribution lines data.....	53
Figure 5.9 Interface for setting the optimization parameters and constraints.....	54

---

Figure 5.10 A screenshot of parameter input screen for the economic and environmental study .....	55
Figure 5.11 Sample result for the GHG emissions of three transport networks .....	56
Figure 5.12 Sample result for the CAPEX/OPEX of three transport networks .....	56

---

## LIST OF TABLES

Table 2.1 YRT Terminals and Bus Routes located on Feeder 12M3 .....	20
Table 2.2 CYME-output summary results.....	25
Table 2.3 Buttonville substation feeders summary .....	26
Table 2.4 Demand increase in Buttonville substation demand.....	26
Table 2.5 Data of on-Board Bus Batteries and Fast Chargers.....	29
Table 2.6 BEBS Energy Consumption Based on Traffic Flow Condition.....	31
Table 2.7 Optimal BEBs Configuration .....	32
<i>Table 3.1: Sample of transit network data for regression analysis .....</i>	<i>37</i>
Table 3.2: The total error of several regression models .....	39
Table 4.1 BEB and Diesel Bus Economic Parameters .....	43
Table 4.2 Annual BEBs Economic Analysis .....	45
Table 4.3 BEB and Diesel Bus GHG Well-to-Wheel Emissions.....	45
Table 4.4 Ontario’s Transit Bus Networks Aggregated Distance and Energy Consumption According to IESO Zones .....	46
Table 4.5 Ontario Aggregated Operation and Maintenance Cost Comparison BEB vs. Diesel Bus according to IESO Zones .....	47
Table 4.6 Ontario Aggregated GHG Emission Comparison BEB vs. Diesel Bus according to IESO Zones .....	47

# 1. Milestone Deliverables

As indicated in the project proposal, the main deliverable of the fifth milestone is to provide the fourth technical report (R4) that includes details with respect to the development of a user-defined toolbox for the optimal design and operation of battery-based electric buses (BEBs). The toolbox is generically developed to integrate models from transit networks and utility grids, as well context-specific profiles that contain simulation parameters (number of buses, number of daily trips etc.). As a result, the toolbox represents a fully-integrated, unified transit-utility optimization platform that includes the appropriate mathematical formulation for buses, bus fleets, charging stations, and utility grids. To improve the usability of the toolbox, a graphical user interface (GUI) is developed to enable a user to define additional parameters, such as: bus fleet data, charging station data, electricity prices, as well as configurable options for adding energy storage features and boundaries of operation/design variables.

An overview of this technical report and the analysis process is depicted in the flowchart shown in Figure 1.1, which is comprised of three modules. The first module calculates energy consumption characteristics such as the energy consumption profile and total average energy consumption for a BEB trip, where the calculation is based on the BEB datasheet and user-specified speed profile as depicted in a previous technical report (R3). The calculated energy consumption characteristics are combined with transit block data (bus schedule and initial battery state of charge) to determine the charging schedule of the bus in Module 2. It is worthwhile to note that a utility-transit optimization model is developed to generate the BEB battery capacity and its charging schedule. Finally, the charging profiles of individual BEBs are aggregated along with electricity usage data and GHG parameters to conduct; 1) a comparison between diesel and BEBs in terms of costs and GHG emissions, and 2) a multiple regression model as a robust analytical tool to exemplify the multidimensional input-output relationships between the transit network characteristics and the designed electric bus system characteristics. The detailed computational models of the three modules are further explained in the following sections.

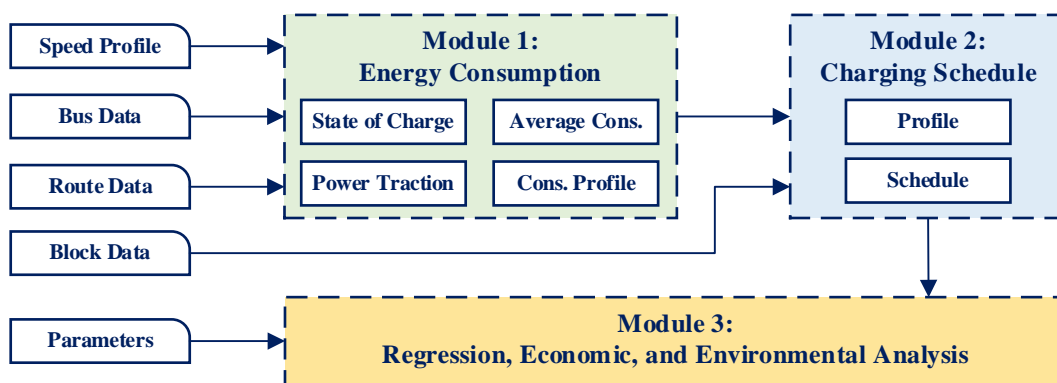


Figure 1.1 Framework of the proposed Transit Electrification Toolbox; where Module 1 is presented in Technical Report R3

---

## 2. Utility-Transit Mathematical Model Formulation

Previous attempts in the design of BEB systems have not adequately explored: (i) developing a mathematical model for electrified transit bus fleets; (ii) incorporating accurate modeling for the energy consumption of BEBs taking into account the route topology, weather conditions, and traffic flow; (iii) considering the operational requirements of power distribution networks; and (iv) defining the optimal configuration of both bus battery packs and chargers. In consideration of these shortcomings, this section introduces a new mathematical model that is developed for BEB fleets in collaboration with Dr. Mohamed at McMaster University [3]. The proposed mathematical formulation is developed for the integrated utility–transit model, which aims at optimizing the BEB system configuration in consideration of battery capacity and the rated size of the chargers. The formulated optimization model minimizes the capital expenditure to electrify a transit bus network, while considering the operational constraints imposed by both power and transit networks. A detailed BEB energy consumption model is also incorporated in the optimal configuration model to enhance its accuracy.

Public bus transit has traditionally been designed to serve the public in relatively dense urban areas, where travel patterns and volumes enable service along fixed routes that follow predetermined schedules. Transit network scheduling is a process that yields a timetable that includes departure times from all the stops served by each route in the network. Each route–based timetable consists of the departure times from the initial terminal, the expected departure times from each bus–stop on the route, and expected arrival times at the final depot. The transit network timetabling is dependent on many factors, which notably include: transit route networks, passenger demand, transfer coordination, and fleet size. Hence, a seamless transition toward electric transit systems necessitates preserving the operation timetable.

Figure 2.1 shows a schematic overview for the proposed utility–transit electrification model. As shown in the figure, the transit network operational schedule is inputted to the BEBs’ transit fleet model. This leads to the identification of transit network electrification parameters that preserve the transit network operational requirements. Also, transit fleet data and network topology (i.e., BEBs’ weight, efficiencies, speed profiles, and routes distance and topography) are inputted to the energy consumption model to calculate the BEBs’ energy consumption in kWh/km. To that end, the output of the BEBs’ transit fleet model and the energy consumption model, in addition to the utility grid data and operational requirements, are inputted to the developed utility–transit model. The utility–transit model aims to determine the optimal configuration for an electric transit city bus fleet, which includes the sizing of the battery capacity of the BEBs, as well as the dimensions of the charging stations, e.g., size and number of chargers.

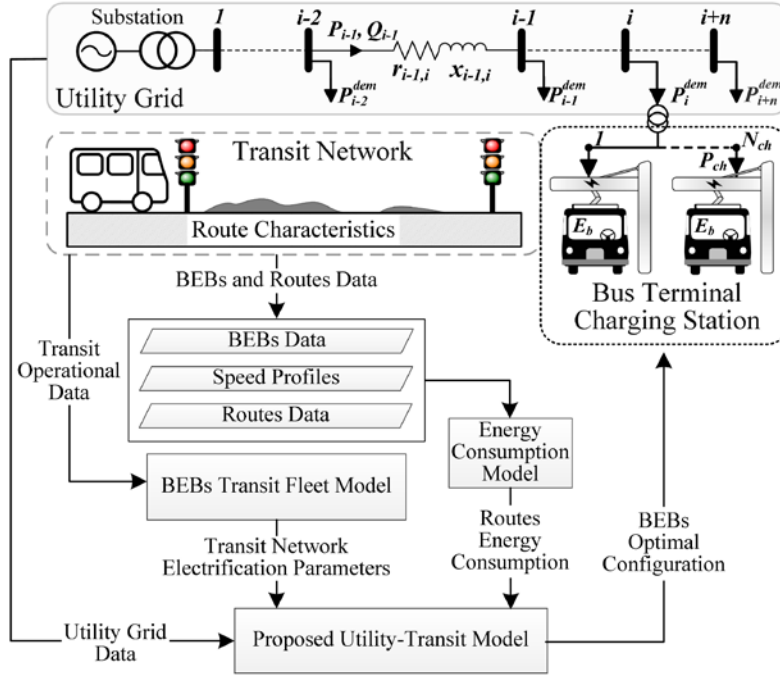


Figure 2.1 Framework for the proposed utility-transit optimization model.

## 2.1 Modeling of Utility-Transit Toolbox

As discussed earlier, a seamless transition towards transit electrification requires the preservation of the operation timetable. Therefore, modeling the BEBs' consumption under the existing transit timetable is essential for satisfying the operational requirements. The bus transit network integrates two components:  $N_b$  number of buses (bus fleet), and  $N_r$  number of routes. Both are represented with identification numbers in the form of sets  $\mathcal{B}$  and  $\mathcal{R}$ , respectively, as:

$$\mathcal{B} = \{1, 2, \dots, b, \dots, N_b\}; \quad (1)$$

$$\mathcal{R} = \{1, 2, \dots, r, \dots, N_r\}. \quad (2);$$

where,  $b$  and  $r$  are indices for BEBs and the transit system routes, respectively. Transit providers assign buses to routes according to their operational trip requirements. Where, the set of BEB  $b$  trip assignments,  $\mathcal{J}_b$ , throughout the operating hours can be given as follows:

$$\mathcal{J}_b = \{1, 2, \dots, j, \dots, N_{b,j}\}, \forall b \in \mathcal{B}; \quad (3)$$

As shown in Figure 2.2, in each assigned trip  $j$ , bus  $b$  is scheduled for route  $r$  for a pre-specified scheduling period ( $S_{b,j}$ ), defined as follows:

$$S_{b,j} = [T_{b,j}^{Dep}, T_{b,j}^{Arr}, \tau_{b,j}^{Trp}, \tau_{b,j}^{Rec}, r_{b,j}, l_{b,j}], \forall j \in \mathcal{J}_b. \quad (4)$$

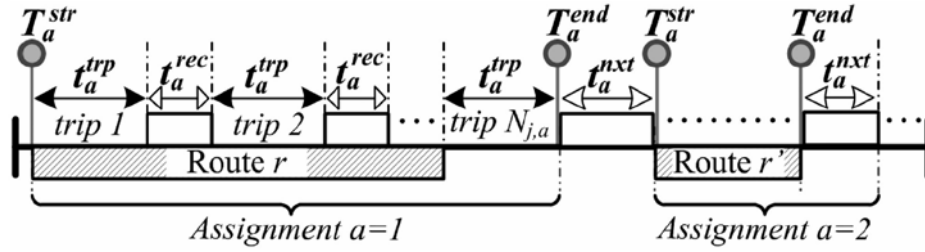


Figure 2.2 Schematic diagram for the transit schedule assignments for a bus  $b$ .

where,  $T_{b,j}^{Dep}$  and  $T_{b,j}^{Arr}$  are the departure and arrival time of BEB  $b$  trip  $j$ , respectively;  $r_{b,j}$  indicates the BEB route at trip  $j$ ;  $\tau_{b,j}^{Trp}$  and  $\tau_{b,j}^{Rec}$  are the trip time, and recovery (i.e., layover) time in minutes for trip  $j$ , respectively; and  $l_{b,j}$  represents the BEB route length, respectively. Sequentially, each bus operates the given number of trips within a pre-specified schedule, where the recovery time represents the bus idling at the bus terminal station after each trip. To that end, the proposed algorithm aims to design the BEB configuration defined as the bus battery capacity, chargers' number and size, and charger's allocation. As such, the objective function of the proposed algorithm optimizes the total BEB electrification cost that is defined as follows:

$$\text{Minimize: } \left\{ \begin{array}{l} \sum_{b \in \mathcal{B}} N_b \cdot E_b \cdot C_b^{Exp,Bat} + \sum_{m \in \mathcal{M}} N_m^{Chr} \cdot P_m^{Chr} \cdot C_m^{Exp,Chr} \\ + \sum_{m \in \mathcal{M}} N_m^{Chr} \cdot C_m^{Ins,Chr} \end{array} \right\}, \quad (5)$$

$$\forall b \in \mathcal{B} \wedge \forall m \in \mathcal{M}.$$

where,  $N_b$ ,  $E_b$ , and  $C_b^{Exp,Bat}$  represents the BEBs' number, battery capacity, and normalized battery expenditure cost, respectively; and  $P_m^{Chr}$ ,  $N_m^{Chr}$ ,  $C_m^{Exp,Chr}$ , and  $C_m^{Ins,Chr}$  represent terminal  $m$  chargers size, charger number, normalized charger expenditure cost, and the charger installation cost, respectively. As depicted in (5) the objective function consists of three terms:

- Cost of the BEBs' battery packs as the product of number of BEBs  $N_b$ , battery capacity  $E_b$  and battery cost  $C_b^{Exp,Bat}$ , as follows:  $\sum_{b \in \mathcal{B}} N_b \cdot E_b \cdot C_b^{Exp,Bat}$
- Cost of the charging infrastructure packs as the product of number of chargers  $N_m^{Chr}$ , charger rating  $P_m^{Chr}$  and charger cost  $C_m^{Exp,Chr}$ , as follows:  $\sum_{m \in \mathcal{M}} N_m^{Chr} \cdot P_m^{Chr} \cdot C_m^{Exp,Chr}$ .
- Cost of charger's installation as the product of charger's number  $N_m^{Chr}$ , and charger installation cost  $C_m^{Ins,Chr}$ , as follows:  $\sum_{m \in \mathcal{M}} N_m^{Chr} \cdot C_m^{Ins,Chr}$ .

To this end, for each bus  $b$  at trip  $j$ , the departure and arrival state of charge (SOC) of the BEB battery are constrained by the SOC limits imposed by the bus manufactures and defined as:

$$SOC_{b,j}^{Dep} \leq SOC_b^{Max}, \forall b \in \mathcal{B} \wedge \forall j \in \mathcal{J}_a; \quad (6)$$

$$SOC_{b,j}^{Arr} \geq SOC_b^{Min}, \forall b \in \mathcal{B} \wedge \forall j \in \mathcal{J}_a; \quad (7)$$

where,  $SOC_{b,j}^{Dep}$  and  $SOC_{b,j}^{Arr}$  are the departure and arrival SOC of BEB  $b$  along trip  $j$ , respectively;  $SOC_b^{Min}$  and  $SOC_b^{Max}$  are the BEB minimum and maximum SOC limits, respectively. As such, the bus manufacturers set those limits to maintain a long battery lifetime and avoid limp issues. Where, the arrival SOC for each bus  $b$  is calculated as:

$$SOC_{b,j}^{Arr} = SOC_{b,j}^{Dep} - 100 \times \frac{E_{b,j}^{Cons}}{E_b} \cdot l_{b,j}, \forall b \in \mathcal{B} \wedge \forall j \in \mathcal{J}_a. \quad (8)$$

Where,  $E_{b,j}^{Cons}$  is the BEB average consumption during trip  $j$ . As such, the battery size is constrained by the minimum capacity,  $E_b^{Min}$ , and the maximum capacity limits,  $E_b^{Max}$ , as follows:

$$E_b^{min.} \leq E_b \leq E_b^{max.}, \forall b \in \mathcal{B}. \quad (9)$$

Equation (5) is also subject to the SOC charging equation upon the arrival of the BEB to the terminal after each trip:

$$SOC_{b,j}^{Dep} = SOC_{b,j}^{Arr} + \Delta SOC_{b,j}, \forall b \in \mathcal{B} \wedge \forall j \in \mathcal{J}_a; \quad (10)$$

$$\Delta SOC_{b,j} = \eta_{ch} \left( \frac{P_m^{Chr} T_{b,j}^{Chr}}{60 \times E_b} \right) \times 100, \quad (11)$$

$$\forall b \in \mathcal{B} \wedge \forall m \in \mathcal{M} \wedge \forall j \in \mathcal{J}_a \wedge \forall m = L_{b,j}^{Trm};$$

where,  $\eta_{ch}$  is the charger efficiency;  $T_{b,j}^{Chr}$  is the BEB charging time in minutes; and  $L_{b,j}^{Trm}$  represents the BEB  $b$  arrival terminal location after a trip  $j$ . As such, (11) shows that the charged SOC depends on the battery capacity  $E_b$ , as well as the charger size  $P_m^{Chr}$  and the charging time  $T_{b,j}^{Chr}$  decision variables, which are constrained to their allowable limits, respectively:

$$P_m^{Min.} \leq P_m^{Chr} \leq P_m^{Max}; \quad (12)$$

$$0 \leq T_{b,j}^{Chr} \leq \tau_{b,j}^{Rec} - \tau^{Pio}, \forall b \in \mathcal{B} \wedge \forall j \in \mathcal{J}_a; \quad (13)$$

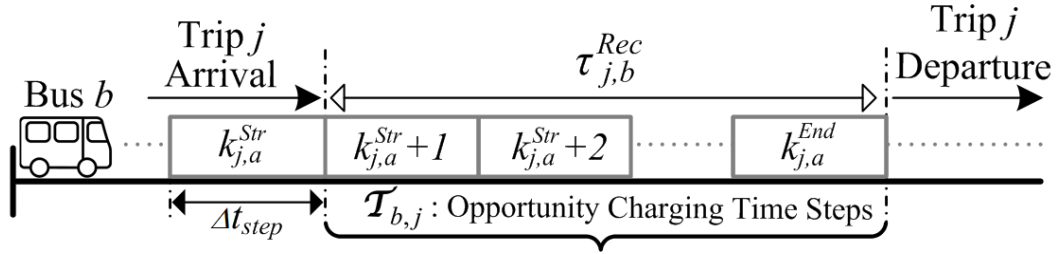


Figure 2.3 Schematic diagram for the BEB charging opportunity after each trip j.

where,  $P_m^{\text{Min}}$  and  $P_m^{\text{Max}}$  are the minimum and maximum charger size limits, respectively; and  $\tau^{Pio}$  is the charger plug-in and plug-out time in minutes. Equation (13) indicates that the maximum charging time limit is equal to the recovery time minus the time for plugging-in and plugging-out the charger.

Equations (6) - (13) constrain the BEBs' SOC and charging time in a trip domain window, and as such, each variable corresponds to a given trip. However, the coordination of the BEBs' charging process at each transit terminal station should be done in a real-time window domain in order to optimally design the charger's number and rating power. For this reason, the transit daily operation,  $\mathcal{T}$ , is divided into equal time steps of  $\Delta t_{step}$ . Where, each transit terminal station has its own  $N_b \times N_t$  opportunity charging matrix that is given as:

$$\begin{pmatrix} M_{m,1}^{Opp}(1) & \dots & M_{m,b}^{Opp}(1) & \dots & M_{m,N_b}^{Opp}(1) \\ \vdots & \vdots & \vdots & \vdots & \vdots \\ M_{m,1}^{Opp}(t) & \dots & M_{m,b}^{Opp}(t) & \dots & M_{m,N_b}^{Opp}(t) \\ \vdots & \vdots & \vdots & \vdots & \vdots \\ M_{m,1}^{Opp}(N_t) & \dots & M_{m,b}^{Opp}(N_t) & \dots & M_{m,N_b}^{Opp}(N_t) \end{pmatrix}, \quad (14)$$

$$\forall b \in \mathcal{B} \wedge \forall t \in \mathcal{T};$$

Equation (14) aims to indicate the intersected charging time of the BEBs at each time step t (i.e. at each row), in order to coordinate their charging process. As such, the algorithm might decide to either increase the number of chargers at the terminal or decrease the BEBs' charging time, in such a way as to satisfy the BEBs' departure and arrival SOC. Where, each matrix element in (14) represents the charging time variable of each BEB at terminal m that is represented as follows:

$$M_{m,b}^{Opp}(t) = \begin{cases} T_{b,j}^{ch.}, & \forall t \in \mathcal{T}_{b,j} \wedge \forall b \in \mathcal{B} \wedge \forall m = L_{b,j}^{Trm}; \\ 0, & \text{Otherwise} \end{cases} \quad (15)$$

where,  $\mathcal{T}_{b,j}$  defines the set of time steps at which the BEB b has the opportunity to charge after a given trip j. As shown in Figure 2.3, a set of charging opportunity time steps is defined after each trip as:

$$\mathcal{T}_{b,j} = \{k_{j,b}^{Str}, k_{j,b}^{Str} + 1, \dots, k_{j,b}^{End}\}, \forall b \in \mathcal{B} \wedge \forall j \in \mathcal{J}_a; \quad (16)$$

$$k_{b,j}^{Str} = 1 + \frac{60 \times T_b^{Dep} + j \cdot \tau_b^{Cyc} - \tau_b^{Rec}}{\Delta t_{step}}, \forall b \in \mathcal{B} \wedge \forall j \in \mathcal{J}_a; \quad (17)$$

$$k_{b,j}^{End} = k_{b,j}^{Str} + \frac{\tau_{b,j}^{Rec}}{\Delta t_{step}} - 1, \forall b \in \mathcal{B} \wedge \forall j \in \mathcal{J}_a; \quad (18)$$

where, the trip cycle time is represented as follows:

$$\tau_b^{Cyc} = \tau_b^{Trp} + \tau_b^{Rec}, \forall b \in \mathcal{B}. \quad (19)$$

Likewise the opportunity charging matrix introduced in (14), each bus terminal  $m$  has a similar matrix  $K_{m,b}^{Str}$  and  $K_{m,b}^{End}$ , which defines the starting and ending time step of  $M_{m,b}^{Opp}(t)$ , respectively. To that end, equation (5) is also subject to the charging coordination constraint as follows:

$$\sum_{t \in \mathcal{T}} M_{m,b}^{Opp}(t) \leq \Delta t_{Step} \left( K_{m,b}^{End^+}(t) - K_{m,b}^{Str^-}(t) + 1 \right) N_m^{Chr}, \quad (20)$$

$$\forall m \in \mathcal{M} \wedge \forall b \in \mathcal{B};$$

$$K_{m,b}^{End^+}(t) = \text{Max.}_{t \in \mathcal{T}} \{K_{m,b}^{End}(t)\}, \forall m \in \mathcal{M} \wedge \forall b \in \mathcal{B}; \quad (21)$$

$$K_{m,b}^{Str^-}(t) = \text{Min.}_{t \in \mathcal{T}} \{K_{m,b}^{Str}(t)\}, \forall m \in \mathcal{M} \wedge \forall b \in \mathcal{B}; \quad (22)$$

Equation (20) states that for the buses that have an intersected opportunity charging time window, their variable charging time summation should be within the product of their aggregated charging opportunity time (i.e.,  $K_{m,b}^{End^+}(t) - K_{m,b}^{Str^-}(t) + 1$ ) and the number of available chargers at the terminal. As such, increasing the number of the chargers in (20), increases the aggregated possible charging time duration as shown in (21). Where, the charger's number are constrained by their minimum limit,  $N_m^{Min}$ , and their maximum limit,  $N_m^{Max}$ , as follows:

$$N_m^{Min} < N_m^{Chr} < N_m^{Max}. \quad (23)$$

Also, the objective function in (5) is subjected to the power distribution system (PDS) voltage constraints derived from (4) as follows:

$$\sum_{m \in \mathcal{M}} \left( P_{m,n',s}^{Chr}(t) \cdot \sum_{n=1}^{n'} r_{s,n} \right) - \left( V_{min} - V_{s,n_e}^{Ini}(t) \right) \leq \varepsilon, \quad (24)$$

$$\forall t \in \mathcal{T} \wedge \forall n \& n' \in \mathcal{N} \wedge \forall m \in \mathcal{M} \wedge \forall s \in \mathcal{S};$$

where (24) constrains the impact of the consumed power at each transit terminal charging station, so as to not violate the end/weakest node among the power networks. As such,  $V_{s,n_e}^{Ini}$  is the initial voltage of the PDS node

prior to the penetration of the electrified transit into the PDS. Also, the objective function in (5) is subject to the feeder's power flow limits given as follows:

$$\left| P_{m,n,s}^{Chr}(t) + P_{s,n'}^{Ini}(t) \right| < P_{s,n'}^{Max}, \quad (25)$$

$$\forall n \& n' \in \mathcal{N} \wedge \forall n' < n \wedge \forall t \in \mathcal{T} \wedge \forall s \in \mathcal{S};$$

where,  $P_{s,n'}^{Ini}$  is the initial power flow of node  $n'$  prior to the integration of the electrified transit system. Equation (25) represents the interdependency constraint between the transit network and the PDS, which is a function of the BEBs' charging power. It is worth noting that the initial voltage and power flow at each feeder/node is obtained by solving the power flow mismatch equation of the PDS as given in (26) - (30), and then they are inputted to the proposed algorithm to be considered in equations (24) - (25).

$$P_{n,t}^{Gen} - P_{n,t}^{Dem} = V_{n,t} \sum_{n' \in \mathcal{N}} V_{n',t} Y_{nn'} \cos(\delta_{n,t} - \delta_{n',t} - \theta_{nn'}), \quad (26)$$

$$\forall n \in \mathcal{N} \wedge \forall t \in \mathcal{T};$$

$$Q_{n,t}^{Gen} - Q_{n,t}^{Dem} = V_{n,t} \sum_{n' \in \mathcal{N}} V_{n',t} Y_{nn'} \sin(\delta_{n,t} - \delta_{n',t} - \theta_{nn'}), \quad (27)$$

$$\forall n \in \mathcal{N} \wedge \forall t \in \mathcal{T}$$

where,  $P_{n,t}^{Gen}$  and  $P_{n,t}^{Dem}$  are the active power generation and demand at node  $n$ , respectively;  $Q_{n,t}^{Gen}$  and  $Q_{n,t}^{Dem}$  are the reactive power generation and demand at node  $n$ , respectively;  $V_{n,t}$  and  $\delta_{n,t}$  are the voltage magnitude and angle at node  $n$ , respectively;  $Y_{nn'}$  and  $\theta_{nn'}$  are the admittance magnitude and angle between node  $n$  and  $n'$ , respectively. Equations (26) and (27) state the active and reactive power mismatch equations, respectively. The objective function stated in (5) is also subjected to the allowable node's voltage limit, as well as the branches' capacity limits as follows:

$$V_n^{Min} < V_{n,t} < V_n^{Max}, \forall n \in \mathcal{N} \wedge \forall t \in \mathcal{T}; \quad (28)$$

$$\left| P_{n,t} \right| < P_n^{Max}, \forall n \in \mathcal{N} \wedge \forall t \in \mathcal{T}; \quad (29)$$

$$V_{s,e}^{Ini}(t) = \min(V_{n,t}), \quad (30)$$

$$\forall n \in \mathcal{N} \wedge \forall t \in \mathcal{T} \wedge \forall s \in \mathcal{S};$$

Where,  $V_n^{Min}$  and  $V_n^{Max}$  are the minimum and maximum PDS voltage limits;  $P_n^{Min}$  and  $P_n^{Max}$  are the minimum and maximum power flow operation requirement.

---

## 2.2 Utility-Transit Model Coding and testing

The CYME Power Engineering Software is used to validate that the optimized BEBs' configuration will not impose any violation on any of the power systems analyzed during the project. In this regard, MATLAB software is used to code and test the proposed utility-transit model. The proposed optimization model is a mixed integer non-linear programming (MINLP) problem. In this work, the proposed formulated optimization problem is solved using the Basic Open-source Nonlinear Mixed Integer programming solver (BONMIN). The BONMIN solver uses a combined Interior Point nonlinear programming and branch and cut linear programming techniques for solving the MINLP optimization problem. Also, it is worth noting that the BONMIN algorithm has the functionality to incorporate heuristic techniques to handle large MINLP problems. In particular, the incorporated heuristic techniques help speeding up the detection of an infeasible solution search path to rapidly find a feasible solution. Due to the non-convexity of the proposed optimization problem given the non-linearity of the imposed set of constraints, a global optimal solution that refers to lowest objective function value across the feasible unknown range cannot be guaranteed. To that end, the BONMIN optimization solver is bundled as a MATLAB built-in function in the Optimization Interface (OPTI) toolbox. Hence, the problem is coded and solved using the OPTI toolbox. The coded optimization algorithm is executed on a PC with the following specifications: Core i7-6700, 3.4 GHz CPU, 16 GB RAM, and 64-bit Windows operating system. The convergence tolerance is set to  $10^{-7}$ , while, the maximum number of iterations, function evaluations and integer solver nodes is set to  $10^4$ .

## 2.3 Numerical Results

Using the provided data by Alectra Utilities for York Region in Ontario, Canada, an analysis is conducted on Feeder 12M3 considering three different ratings for the chargers to be connected to the feeder for the purpose of on-route fast DC charging. It has been concluded that while the power distribution system may not impose constraints on the design of BEBs' chargers, using smaller charger ratings would have a smoother impact on the power system as will be discussed in Section 2.3.1.1. In Section 2.3.1.2, the impacts of the BEBs' charging profile on the substation capacity are evaluated. In Section 2.3.1.3, an energy storage system has been designed to minimize the demand fluctuation of the BEBs' charging. Moreover, to validate the proposed transit-utility model, the city of Belleville is chosen to show the impact of PDS characteristics on the generated BEB configuration (Section 2.3.2).

### 2.3.1 Impact of on-Route Bus Charging on Alectra's Feeders

Using CYME Power Engineering Software, a load flow analysis is conducted for the City of Vaughan in Ontario to assess the impact of electrifying the York Region Transit (YRT) network. In particular, YRT bus terminals are mapped to their nearest three-phase power distribution feeder using the longitude and latitude data for each of the charging stations and the 3-phase nodes in the electric network. Feeder 12M3 is identified as the most penetrated feeder with YRT bus charging stations as shown in Table 2.1, and is chosen as the representative feeder for the analysis. On the feeder, there are seven potential stops that can be equipped with electric bus chargers.

*Table 2.1 YRT Terminals and Bus Routes located on Feeder 12M3*

YRT Charging Stations	Bus No.	YRT Route Names
Kennedy Rd. & Major Mackenzie	42/204	Southbound to Unionville GO Station, northbound to Major MacKenzie Dr
Main St. & Eastern Gate	9	Northbound
Major MacKenzie & Ridgecrest Rd.	9	East loop
Markham Stouffville Hospital	15	Westbound to Yonge St., eastbound to Stouffville
Millard St. & Automall Blvd.	50	Northbound to Sutton/Pefferlaw, southbound to Newmarket GO Bus Terminal
Parkview Village	16	Westbound to Bathurst St, eastbound to Markham Stouffville Hospital
	18	Westbound to Angus Glen Community Ctr, eastbound to Markham Stouffville Hospital
	25	Westbound Weekdays to Harding Blvd. W., eastbound to Markham Stouffville Hospital
Pefferlaw Fire Hall	8	Southbound to Steeles Avenue, northbound to Major Mackenzie Drive

### 2.3.1.1 Impact of BEBs Charging on Feeder’s Loading

Using the Utility-Transit model developed earlier, the charging profiles of the electric buses allocated to be connected to feeder 12M3 at different charging size scenarios are obtained and depicted in Figure 2.4 using a time-resolution of one-minute. The charger sizes are 300 kW, 450 kW, and 600 kW. In addition, the maximum and average hourly demand profiles obtained from historical data for feeder 12M3 are shown in Figure 2.5 for a 24-hour duration. Figure 2.5 shows that feeder’s peak demand increases in the morning from around 7MW at 6:00 to a maximum of 14MW at 18:00 before decreasing during the night.

In order to compare the impact of chargers to be connected to Feeder 12M3, their calculated profiles are converted into one-hour resolution and are depicted in Figure 2.6 and Figure 2.7 for the hourly peak and average charging demand, respectively. The difference between the hourly average and hourly peak charging arises from the fact that opportunity electric buses charge with a high draw of power demand for a few minutes at a time. The figures show that using the lower rating charger will have lower intermittency in the demand as compared to a higher charger rating. For example, as shown in Figure 2.6, the peak charging demand when using a 300kW charger varies between 1.2MW and 1.8MW during 24-hours, whereas the peak demand of 600kW charger varies between 1.3MW and 2.6MW for the same period.

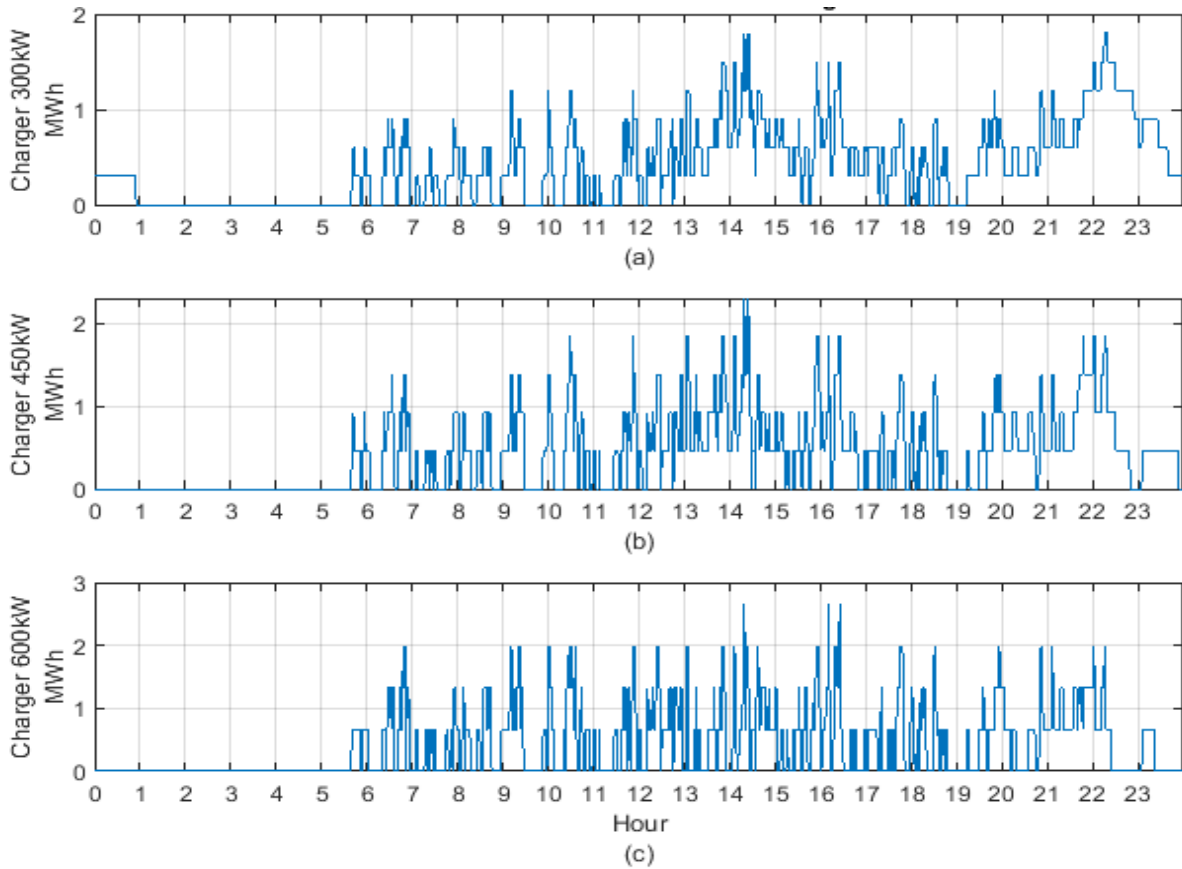


Figure 2.4 Calculated One-minute Resolution of Demand Profiles for Different Size Chargers Connected to Feeder 12M3: (a) 300 kW, (b) 450 kW, and (c) 600 kW Chargers.

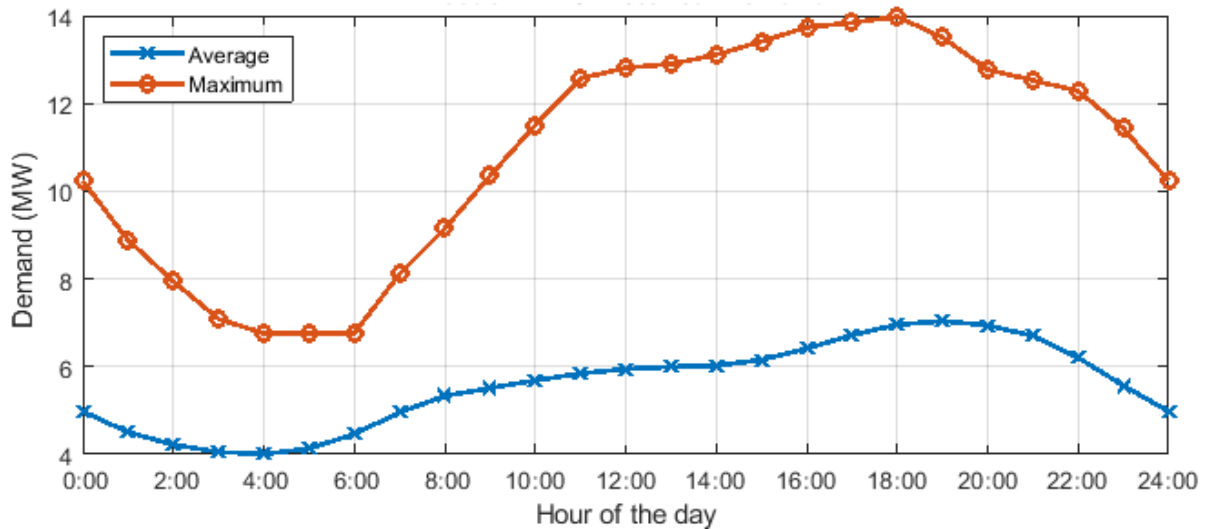
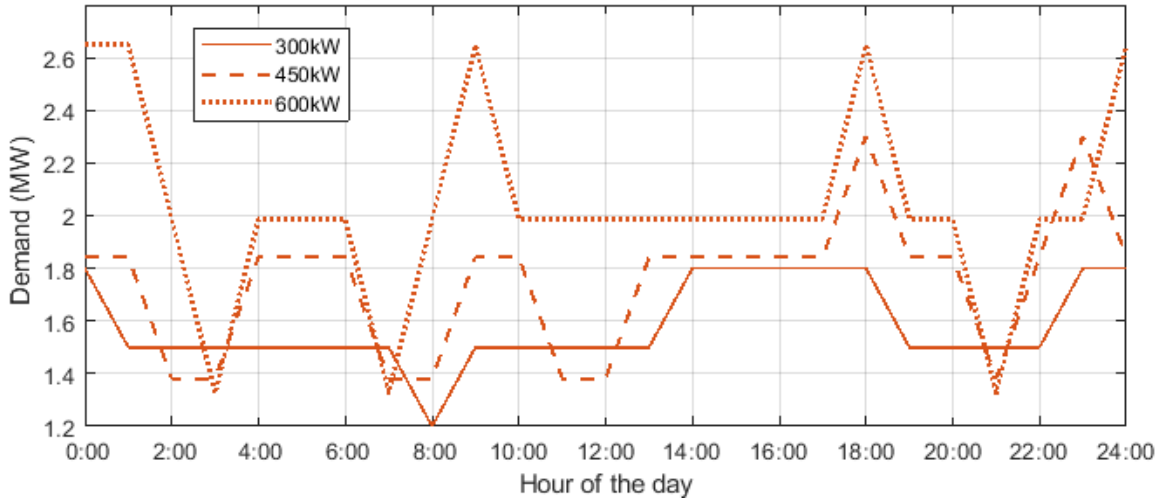
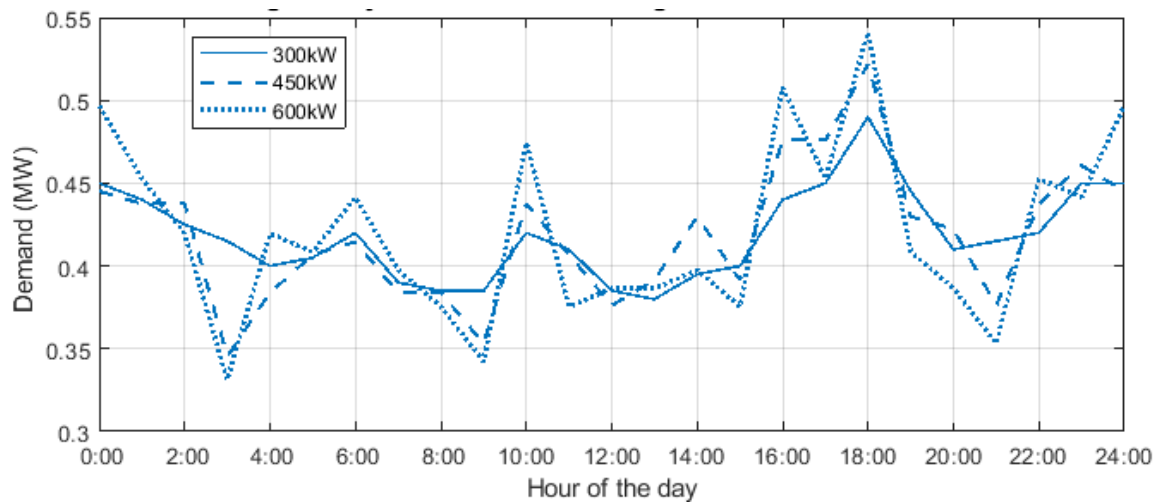


Figure 2.5 Feeder 12M3 Hourly Historical Demand Profile



**Figure 2.6: Hourly peak demand for three different charger ratings to be connected to Feeder 12M3**



**Figure 2.7: Hourly average demand for three different charger ratings to be connected to Feeder 12M3**

A similar observation can be seen for the average demand depicted in Figure 2.7, however the variation range is smaller, (380kW to 490kW) and (330kW to 540kW) for the 300kW and 600kW chargers, respectively.

Combining both the historical demand of Feeder 12M3 and the calculated demand of the chargers to be connected to the feeder reveals the expected increase in the feeder’s demand due to BEBs’ charging. Presumably, the worst-case occurs when the peak of electric bus charging demand coincides with the peak historic demand of Feeder 12M3. For this purpose, the maximum recorded charging demand of the minute resolution charging profile within a specified hour is considered to coincide with the historical feeder’s hourly peak demand. Consequently, the amount of the increase in the peak demand is depicted in Figure 2.8, whereas Figure 2.9 presents the percentage of that increase. The figures illustrate that the peak demand will consistently increase during all hours of the day, causing the maximum peak at 18:00 to rise from 14MW without chargers to 15.8MW, 16.3MW, and 16.6MW when connecting 300kW, 450kW, and 600kW chargers, respectively.

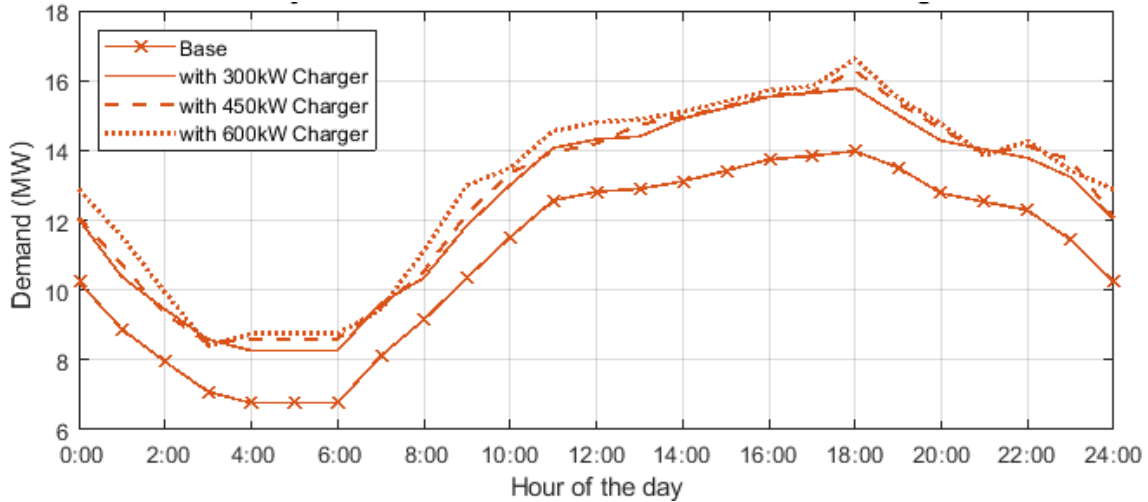


**Figure 2.8: Expected hourly peak demand increase in Feeder 12M3 with three different charger ratings**

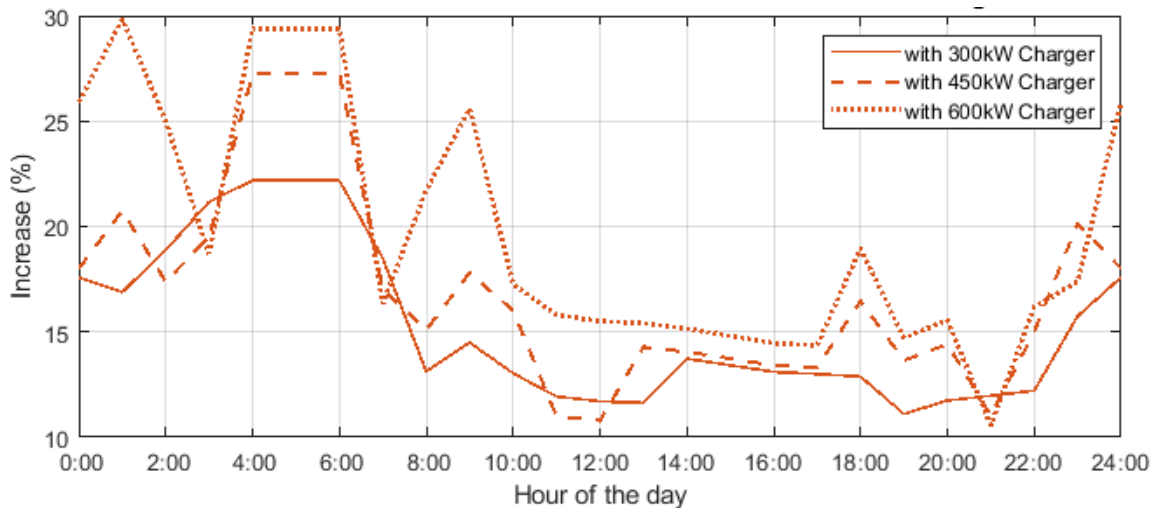


**Figure 2.9: Expected hourly peak demand percent increase in Feeder 12M3 with three different charger ratings**

The percentage of demand increase shown in Figure 2.9 indicates that using chargers with smaller ratings will have a smoother impact on the feeder as compared to using chargers with a higher rating. Specifically, the range of peak demand increases when using a 300kW charger is between 11% to 22% as compared to a range of 10% to 30% when using 600kW charger.

Furthermore, a similar analysis is conducted using the average demand profiles for scenarios with and without the chargers being connected to Feeder 12M3. The results are presented in Figure 2.10 and Figure 2.11, and show a similar trend as was observed for peak demand. The hourly average demand is expected to increase between 5.9% and 10.2% when using 300kW chargers as compared to 5.3% and 10.5% when using 600kW chargers. The results also indicate that there will be no changes to the specific hour of peak demand. Interestingly, the percentage of demand increase during the nighttime, i.e. from 22:00 to 6:00, is higher when compared to the rest of the day.

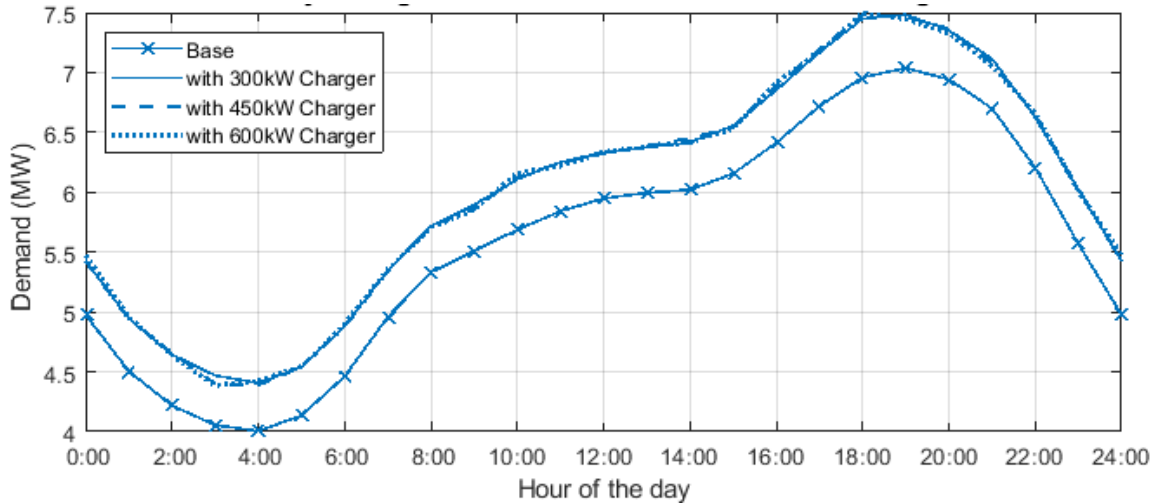


Figure 2.10: Expected hourly average demand increase in Feeder 12M3 with three different charger ratings

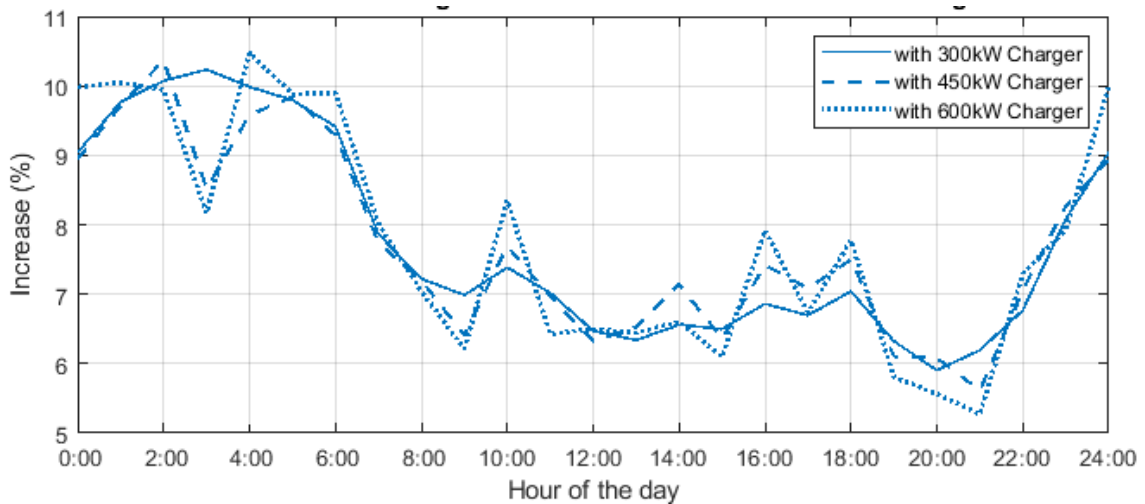


Figure 2.11: Expected hourly average demand percent increase in Feeder 12M3 with three different charger ratings

### 2.3.1.2 Impact of BEBs Charging System on the Voltage Profile and Losses

This subsection explores the impact of the charging profile on the feeder's voltage, while power losses are also evaluated. In the first step, historical data of the feeder's maximum hourly demand is used to execute a load allocation setup in order to distribute the demand on the various loads connected to the feeder. Also, the source voltage is fixed to 1.0 p.u. during the study to fairly compare the impact on the voltage regardless of the operation of voltage regulators. In the second step, load flow analysis is conducted for the base case (without the connected chargers). Following the base case analysis, the BEBs' charging profile is added to specific locations and the load flow analysis is run again (with chargers) using the exact load allocation as in the base case. The resultant voltage profiles of the two scenarios (i.e., with and without BEBs chargers) are presented in Figure 2.12. As depicted in the figure, the BEBs charging profile does not have any noticeable impact on the voltage profile. A summary of the analysis is presented in Table 2.1, which was generated using CYME. As such, the BEBs' charging profile slightly increases the apparent power losses from 1,012 kVA to 1,046 kVA (an increase of 3.34%).

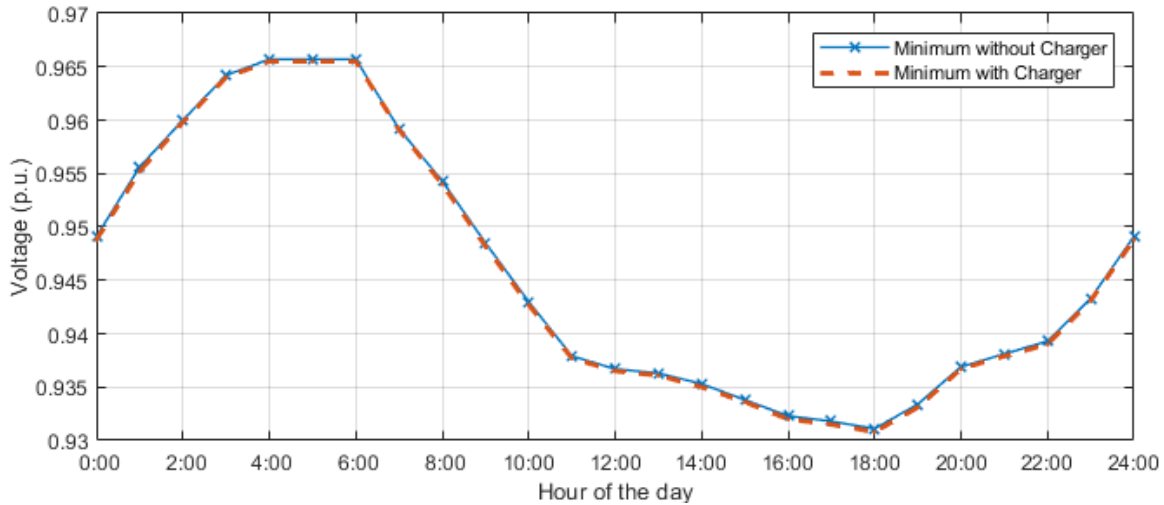


Figure 2.12: Hourly Feeder 12M3 Minimum Voltage with and without Chargers

Table 2.2 CYME-output summary results

		Base Case	With Charger
		Annual Peak	Opportunity
Feeder Loading	Total Load (kVA)	13,810	16,105
	Total Load (kW)	13,102	15,502
	Total Load (kVar)	4,364	4,364
	Overall PF(%)	94.87	96.26
Voltage (p.u.)	Substation	1.00	
	Max Value	0.9964	0.9959
	Min Value	0.9311	0.9308
Losses	Total Losses (kVA)	1,012	1,046
	Total Losses (kW)	417	427
	Total Losses (kVar)	923	955
Operational State	Status	Normal	Normal
	# Buses outside Limits	0	0
	# Overloaded Lines and Cables	0	0
	# Overloaded Transformers	0	0

The results indicate that the voltage in Alectra’s power distribution system in Vaughan area is unlikely to be impacted after the electrification of the YRT transit network as most of the feeders are operating way below their capacities. This finding is limited only to chargers allocated to provide on-route charging for YRT buses. However, considerations of electrifying other buses in the city e.g., GO and school buses might impact these findings. Also, it is expected that the high demand fluctuation in the electrified transit network charging profile will impact the power quality due to the high intermittency of electric demand caused by the on-route fast DC charging of BEBs. For this reason, in Section 2.3.1.4, a study was carried out to size a fast response ESS to eliminate such power fluctuations.

### 2.3.1.3 Impact of BEBs Charging on the Substation Capacity

In the previous section, it was shown that charging BEBs from the power distribution network would increase the demand on the network feeders from a range of 7.75% (considering the average demand profile), to as high as 15.3% (using 300kW chargers). This poses the question whether the upstream distribution substation will be

able to supply the additional power demand due to BEBs' charging without increasing the substation capacity. In this section, the impact of the aggregated chargers on the substation capacity is analyzed considering the Buttonville substation in Markham, Ontario, as an example.

**Table 2.3 Buttonville substation feeders summary**

Feeder	1	2	3	4	5	6	7	8	9	10	11	12	Total
Average (MW)	5.5	0.0	5.4	8.4	8.7	8.4	8.6	6.3	4.8	4.8	0.0	5.4	66.4
Peak (MW)	15.8	5.8	14.0	26.1	20.6	23.4	21.8	21.0	12.8	12.6	6.4	16.6	130.0
Charging units	2	0	7	2	0	3	3	1	0	1	0	1	20

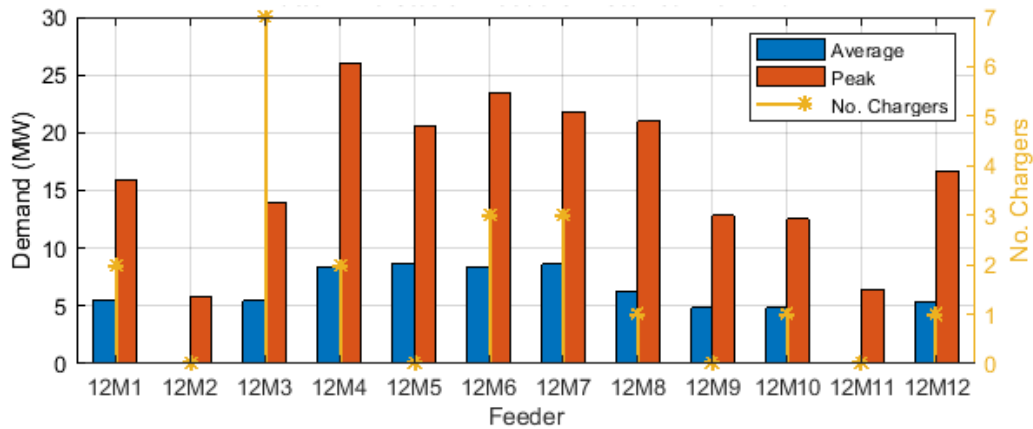


**Figure 2.13: Historical demand of Buttonville substation feeders'**

**Table 2.4 Demand increase in Buttonville substation demand**

Calculation Method	Demand Increase (MW)
1) Maximum Charger's Demand	
300kW	6
450kW	9
600kW	12
2) Average Demand of 0.5 MW/Feeder	4

With 170MVA capacity, the Buttonville substation supplies 12 feeders of Alectra's network as summarized in Table 2.3 and Figure 2.13. Using historical data for the substation, the peak demand of the substation is recorded at 130 MW and the average demand is approximately 66.4 MW, which corresponds to utilization rates of 76.5% and 39%, respectively. Based on the study conducted in the previous sections, the number of BEB chargers to be connected to the Buttonville feeders is identified and are reported in Table 2.3. Out of the 12 feeders, four feeders do not have any chargers connected, while the remaining feeders supply a total of 20 chargers.

Both the maximum and the average total chargers' demand are considered to quantify the increase in demand on the substation due to BEBs' charging. The results are shown in Table 2.4, where the increase in total demand ranges between 4 MW (with 300 kW chargers) and 12 MW (with 600 kW chargers). This translates into increased utilization rates as 41.4% and 83.5% for the average and peak demands, respectively.

### 2.3.1.4 Design of Energy storage for Power Intermittency Minimization

From the study conducted in Section 2.3.1.2, it was found that the charging of BEBs imposes high levels of demand intermittency on the utility grid, where the fluctuation magnitude is highest in the case of opportunity charging. This is due to the nature of opportunity charging since it involves charging the BEBs in short bursts with highly rated chargers. Thus, a fast response energy storage system (ESS) may be needed to eliminate such high levels of fluctuation. In such a case, a super capacitor ESS, which is known for its ability to provide fast response, can eliminate such fluctuations. The impact of the ESS on the fluctuation of the demand can be seen in Figure 2.14 (a), where the “smoothed” plot represents the resultant demand of the charging profile after the ESS has been deployed. Furthermore, the ESS operation (in MW), can be seen in Figure 2.14 (b), which shows the ability of the ESS to provide extremely quick responses to the fluctuation of the demand. Figure 2.14 (c) presents the ESS state of energy for YRT electrified transit network using a 600kW charger. Also, Figure 2.15 (a) presents the super capacitor ESS hourly average consumption. The positive value in the figure signifies the consumed energy that is injected to the system to supply the demand of the BEBs, while the negative values signify the charging of the ESS. Figure 2.15 (b) presents the hourly state of charge for the ESS.

As shown in the figure the SoC of the ESS is always within the allowable operation range, which was set between 10% and 90%. The difference between the original and the smoothed charging profile is the result of the ESS operation, which is shown in Figure 2.14 (b). The figure clearly shows the ability of the ESS to minimize the power demand fluctuation of the BEBs by absorbing/injecting the requisite amount of power from/to the power distribution system.

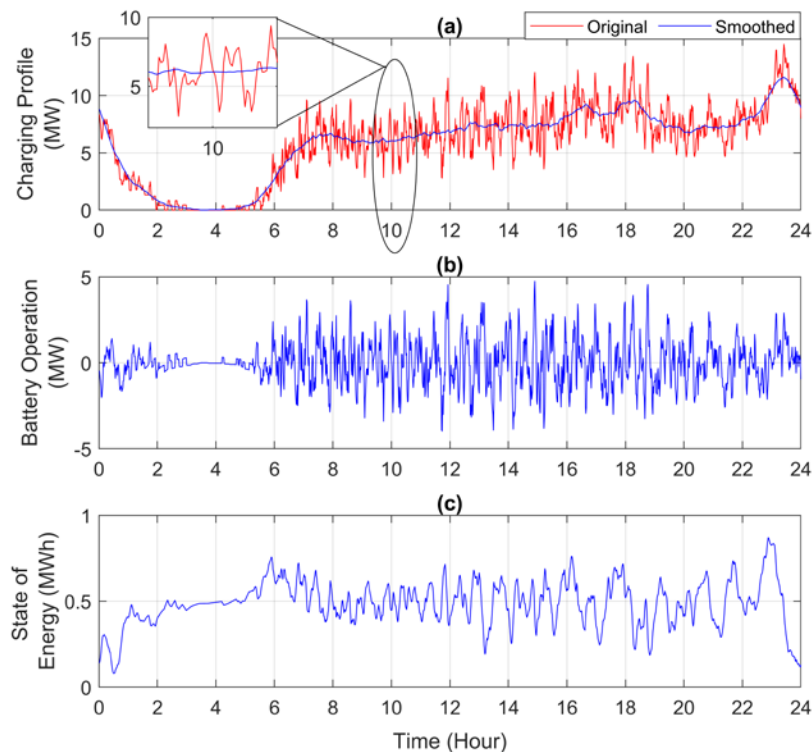


**Figure 2.14** YRT transit network charging profile using 300 kW charger and ESS for profile smoothing: (a) charging profile, (b) ESS operation, and (c) ESS state of energy

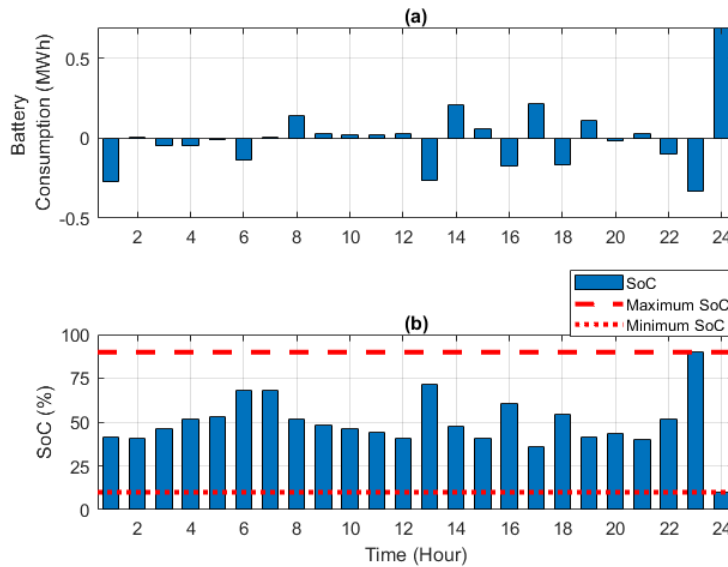


Figure 2.15 YRT transit network ESS for charge smoothing: (a) consumption, and (b) State of charge.

### 2.3.2 Case Study for Belleville Transit Electrification

In order to validate the proposed transit-utility model, a small transit network in Belleville, Ontario is selected as an example of single terminal (hub) based network. Due to the unavailability of the PDS data at Belleville, the data of the well-known 33 bus benchmark PDS was utilized in this study. The use of Belleville transit network and the 33-bus benchmark distribution system aims at shedding the light on potential cases at which careful consideration should be given to both transit and power grids in the configuration design of the electrified bus fleet. Figure 2.16 shows a schematic diagram for the integrated utility-transit system that is utilized to test the accuracy of the proposed model. As shown in the figure, the studied integrated utility-transit system includes a 33-bus PDS coupled with a transit bus network at node 10, in addition to the transit network weekday operation timetable (a real-world representation for Belleville). For the purpose of this study, the transit network is assumed to be fully electrified i.e., all diesel buses are replaced by BEBs. The charging station of the BEBs are located at the bus terminal, which is located at the city center. In this context, the charging station is assumed to be connected to node 10, which is the PDS center load. Figure 2.17 shows a typical daily load profile that is adopted for the studied PDS system loads i.e., without the BEBs. The acceptable voltage deviation was considered as per the American National Standards Institute Range A (i.e., +/- 5%). Table 2.5 shows the input parameters for the bus batteries and the fast chargers, where the time resolution of the studied utility-transit model is 5 minutes.

Given the temporal variation in the traffic flow characteristics, the speed profile is not constant during the scheduled trips. Therefore, three traffic flow conditions, using the ratio ( $v/c$ ) of traffic volume ( $v$ ) to roadway practical capacity ( $c$ ), are considered to accommodate the temporal variation in traffic conditions. These traffic conditions are denoted as free flow, light, and congested traffic. In addition, the speed profile of each bus under each traffic flow condition is calculated and aggregated for the transit network.

**Table 2.5 Data of on-Board Bus Batteries and Fast Chargers**

$SOC_b^{min} = 20\%$	$SOC_b^{max} = 90\%$
$E_b^{min} = 75$ (kWh)	$E_b^{max} = 500$ (kWh)
$P_{ch}^{min} = 75$ (kW)	$P_{ch}^{max} = 500$ (kW)
$N_{ch}^{min} = 1$	$N_{ch}^{max} = 6$
$t^{pio} = 2$ (minutes)	$C_b^{exp} = 300$ (\$/kWh)
$C_{ch}^{inst} = 450$ (\$/kW)	$C_{ch}^{exp} = 35,000$ (\$/charger)
BEB GVWR = 17,200 (kg)	$P_{b,t}^{aux} = 15$ (kW)

GVWR: Gross vehicle weight rating

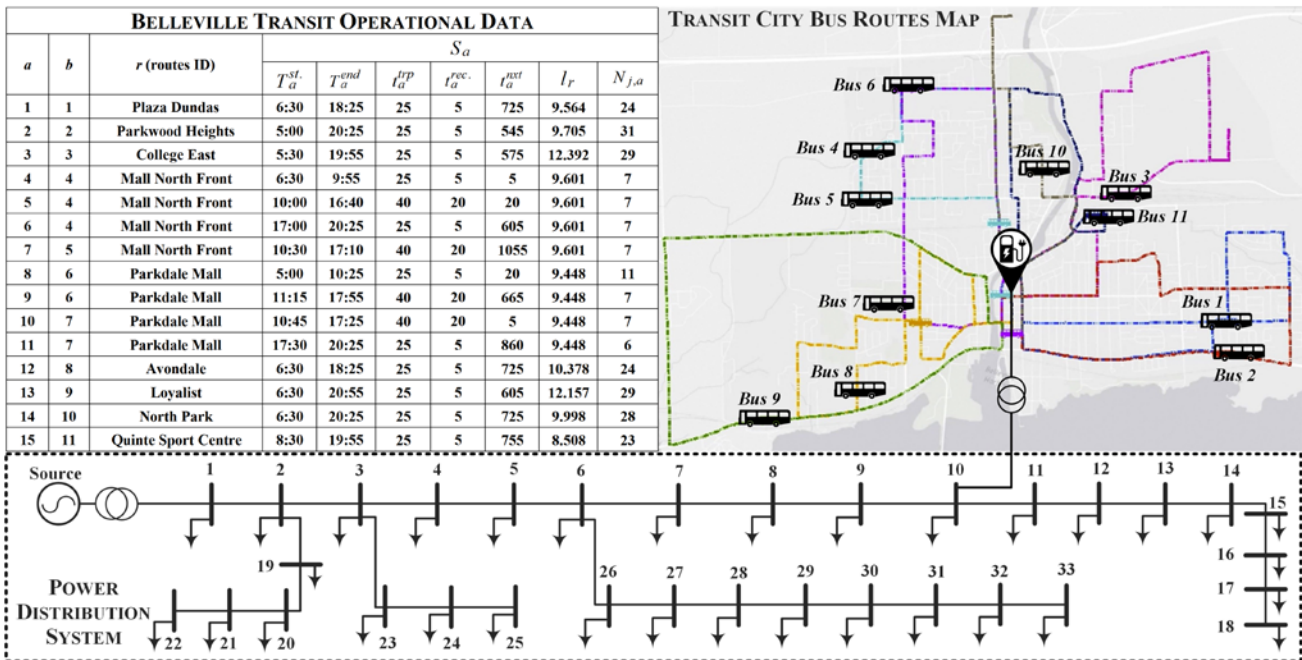


Figure 2.16 Belleville city bus transit map, BEBs assignments data, and its integration with the 33-power distribution system.

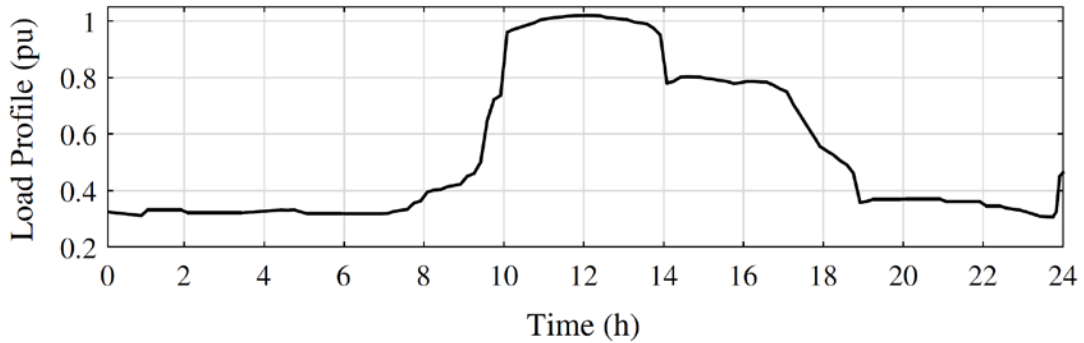
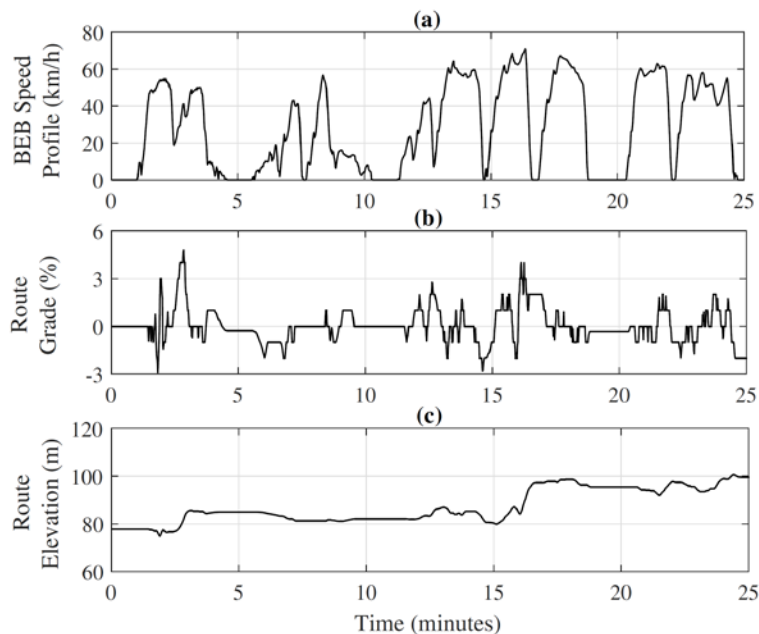


Figure 2.17 Typical daily load profile for the studied system.

To that end, two scenarios are carried out in this work to determine the optimal BEBs' configuration for the studied transit network. Scenario 1 is the base-case scenario, where neither the utility model, nor the traffic conditions are considered. In this scenario, the rate of energy consumption of the BEBs is assumed to be fixed at an average of 1.05 kWh/km as claimed by most bus manufacturers. Scenario 2 represents the proposed integrated model that accounts for traffic flow conditions and the utility operational requirements stated in (25)–(30). The BEBs' energy consumption models are calculated using the Advanced Vehicle Simulator (ADVISOR) according to the manufacturer technical specifications, routes topology, trips time frame, and the corresponding traffic flow conditions. ADVISOR is a simulation tool for vehicle modeling developed by the National Renewable Energy Laboratory (NREL). In order to accurately calculate the energy consumption in Scenario 2, the BEB speed profile, route topography, and auxiliary loads rating should be inputted to the BEBs' energy consumption model. For instance, Figure 2.18 (a)–(c) show the elevation and gradient for the Loyalist route (one of Belleville city bus transit routes shown in Figure 2.16) and the speed profile for its assigned BEB in a congested traffic condition, respectively. Figure 2.19 (a) shows the corresponding power consumption in Scenario 2 for the simulated trip. It is noted that the positive power consumption in Figure 2.19 (a) refers to the drawn power from the BEB energy storage units to drive the BEB and supply the auxiliary loads, while the negative power represents the recovered power during deceleration. Figure 2.19 (b) shows the BEB SOC in both scenarios (i.e., Scenario 1 and Scenario 2) for the simulated trip. As depicted in the figure, the first scenario's representation of the SOC is linear as it lacks the route characteristics, while in the second scenario, the representation of the SOC reflects the route topography and speed characteristics. The simulation has been conducted for all eleven routes at the three traffic conditions i.e., free flow, light, and congested traffic.



**Figure 2.18 Scenario 2: (a) Speed profile, (b) gradient, and (c) elevation, for Loyalist route.**

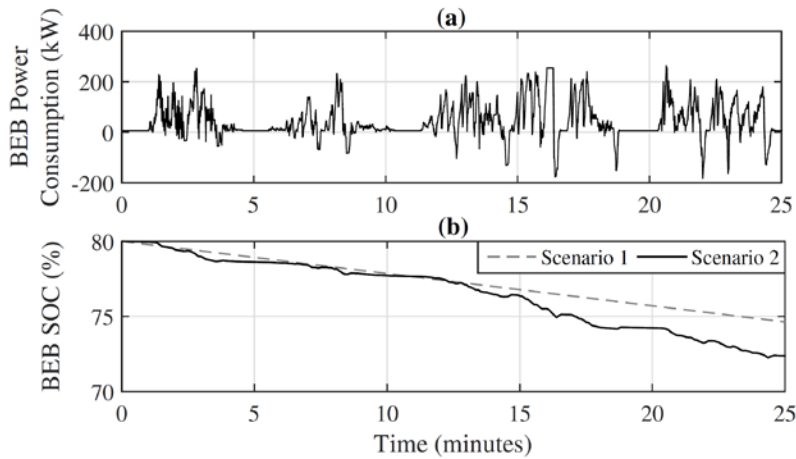


Figure 2.19 BEB #9 operated at Loyalist route (a) scenario 2 energy consumption, and (b) scenario 1 and scenario 2 SOC.

Table 2.6 BEBS Energy Consumption Based on Traffic Flow Condition

Parameters	Free Traffic ( $v/c = 0.35$ )	Light Traffic ( $v/c = 0.55$ )	Congested Traffic ( $v/c = 0.92$ )
Consumption (kWh/km)	0.825	1.1	1.65
Time frame (h)	20:00–7:00	9:00–15:00, 18:00–20:00	7:00–9:00, 15:00–18:00

Table 2-6 shows the average rate of energy consumption for the studied transit network under different traffic conditions. It should be noted that the uncertainty associated with weather conditions is not considered in the model, and the resultant energy consumption is aggregated at the route level. The aggregation of the energy consumption for the transit network is essential from the transit agencies point of view to be able to standardize their fleet of BEBs. Therefore, the BEBs can be scheduled to serve any of the transit system routes. The data in Table 2-6 is inputted to the proposed optimization model. Further, a sensitivity analysis between the feasible BEBs configuration is carried out for the studied scenarios. This is to concisely evaluate: 1) the impact of integrating the PDS model; and 2) quantify the trade-off relation between the BEBs’ optimal configurations.

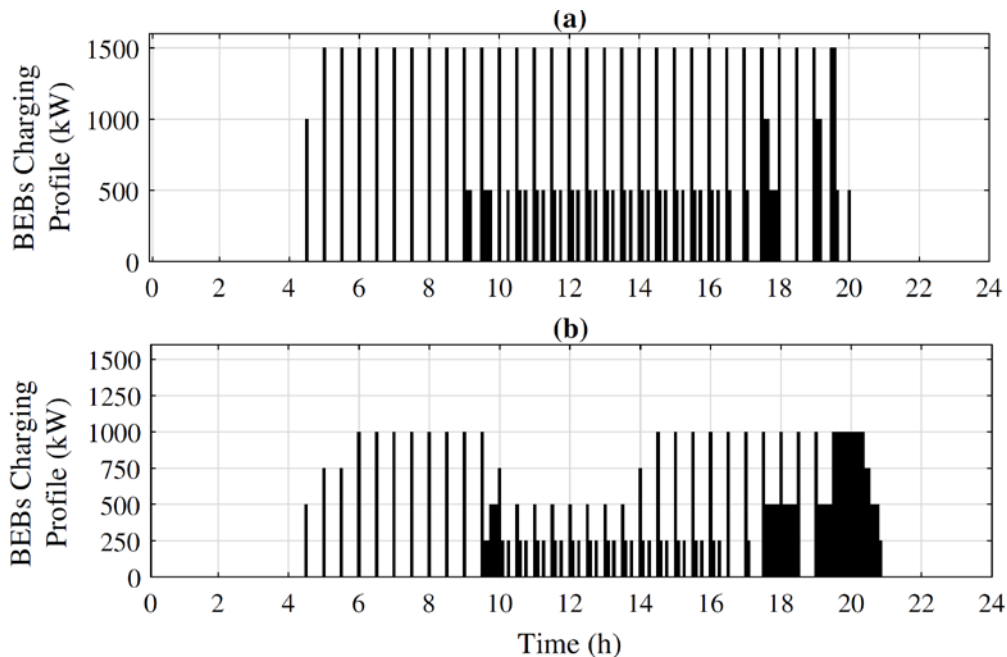
### 2.3.2.1 Optimal BEBs configuration

Table 2-7 shows the optimal configuration of the BEB system for the studied transit network in the two scenarios. The table also shows the cost of each configuration and the total daily consumed energy by the electric bus transit network. As such, accounting for the PDS and the traffic flow conditions (Scenario 2) requires an increase of the net transit electrification cost by 53.8% as compared to Scenario 1 in order to satisfy the scheduled transit operation. It is also noticed that accurate consideration of the traffic flow conditions increases the BEBs’ fleet energy consumption by almost 21%. Figure 2.20 (a)–(b) show the BEBs’ charging profile of the two studied scenarios. Further, the impact of BEBs’ charging on the PDS voltage profile is shown in Figure 2.21, which represents the minimum voltage magnitude across the entire PDS at each time step. As depicted in the figure, without considering the PDS in the design of the BEB configuration, an undervoltage occurs due to the scheduled charging of the BEBs during peak loading conditions. Figure 2.20 (b) and Figure 2.4, however, show that the

proposed integrated model adapted the BEBs configuration and their charging profile in such a way as to not violate the prescribed voltage limit of the PDS. For this reason, the required charger size in Scenario 2 is found to be 250 kW compared to 500 kW in Scenario 1, as shown in Table 2.7. Yet, in order to maintain the scheduled operation of the transit network, the decrease in the charger size requires an increase in the BEBs' battery from 75 to 300 kWh. With a larger battery capacity, BEBs could complete a few consecutive trips without the need of being fully charged. In addition, as illustrated in Figure 2.20, BEBs with larger battery capacities require more time to be fully charged after the completion of their daily assignments to prepare for the next day trips. The results also show that although the charger size in Scenario 2 is decreased (compared to Scenario 1), the available chargers are not fully utilized during heavy-loading conditions of the PDS. For example, during the time of 10:00 to 14:00, only two chargers at a time can be utilized out of four available chargers as shown in Figure 2.20 (b).

**Table 2.7 Optimal BEBs Configuration**

Scenario (ID)	$\mathcal{N}_{ch}$	$\mathcal{P}_{ch}$ (kW)	$\mathcal{E}_b$ (kWh)	Cost (k\$)	Trips consumption (MWh)
Scenario (1)	3	500	75	1027.5	2.65
Scenario (2)	4	250	300	1580	3.21



**Figure 2.20 The BEBs charging profile at; (a) Scenario 1, and (b) Scenario 2.**

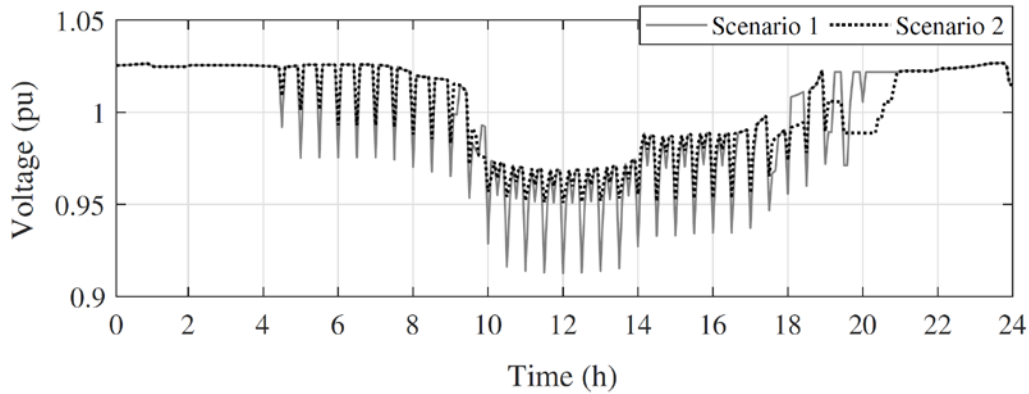


Figure 2.21 The PDS-wide minimum voltage profile for the studied scenarios.

### 2.3.2.2 Sensitivity Analysis of the BEBs Configurations

The results of the above subsection show that there is a trade-off between the choices of the BEB battery capacity and the charger size for a transit network. To that end, a sensitivity analysis is conducted in this section using the proposed optimization model for the two studied scenarios. Given that the BEB battery capacity is modular, different battery capacities with a 25 kWh unit interval are considered for the sensitivity analysis. Figure 2.22 (a) and (b) show the optimal configurations for the electrified transit city bus at different number of chargers for Scenarios 1 and 2, respectively. As shown in Figure 2.22, the relation between the required battery capacity and the required charger size is inversely proportional i.e., the battery capacity decreases with the increase of the charger size. As shown in Figure 2.22 (a), the maximum required battery capacity is found to be 425 kWh for three 75 kW chargers. Figure 2.22 (b), however, shows that the maximum battery capacity for Scenario 2 is 500 kWh at 75 kW charger size for three chargers and above. Hence, in the latter scenario, increasing the number of chargers at 75 kW rated power does not reduce the required battery capacity. As such, a 500 kWh is required for the BEBs' battery capacity, such that the BEBs can deliver the assigned transit schedule given the low charger size of 75 kW. This is mainly because the lower charger size cannot provide sufficient energy to the BEBs during the recovery time. Therefore, a large battery capacity is needed, thereby increasing the probability of BEBs' charging opportunity (i.e. number of chargers).

It is also noticed that the BEBs' battery capacity in Scenario 2 is always higher than Scenario 1 because of the inability of the PDS to provide charging supply to the BEBs during high loading conditions. Therefore, larger battery capacity is required in order to satisfy the transit schedule and BEBs' SOC constraints without violating the PDS constraints. For instance, the results show that only a 75 kWh battery is required for three 500 kW chargers in Scenario 1's optimal configuration as shown in Figure 2.22 (a). However, as depicted in Figure 2.22 (b), the required battery capacity for three 500 kW chargers is found to be 300 kWh for scenario 2 due to the imposed constraints of the PDS.

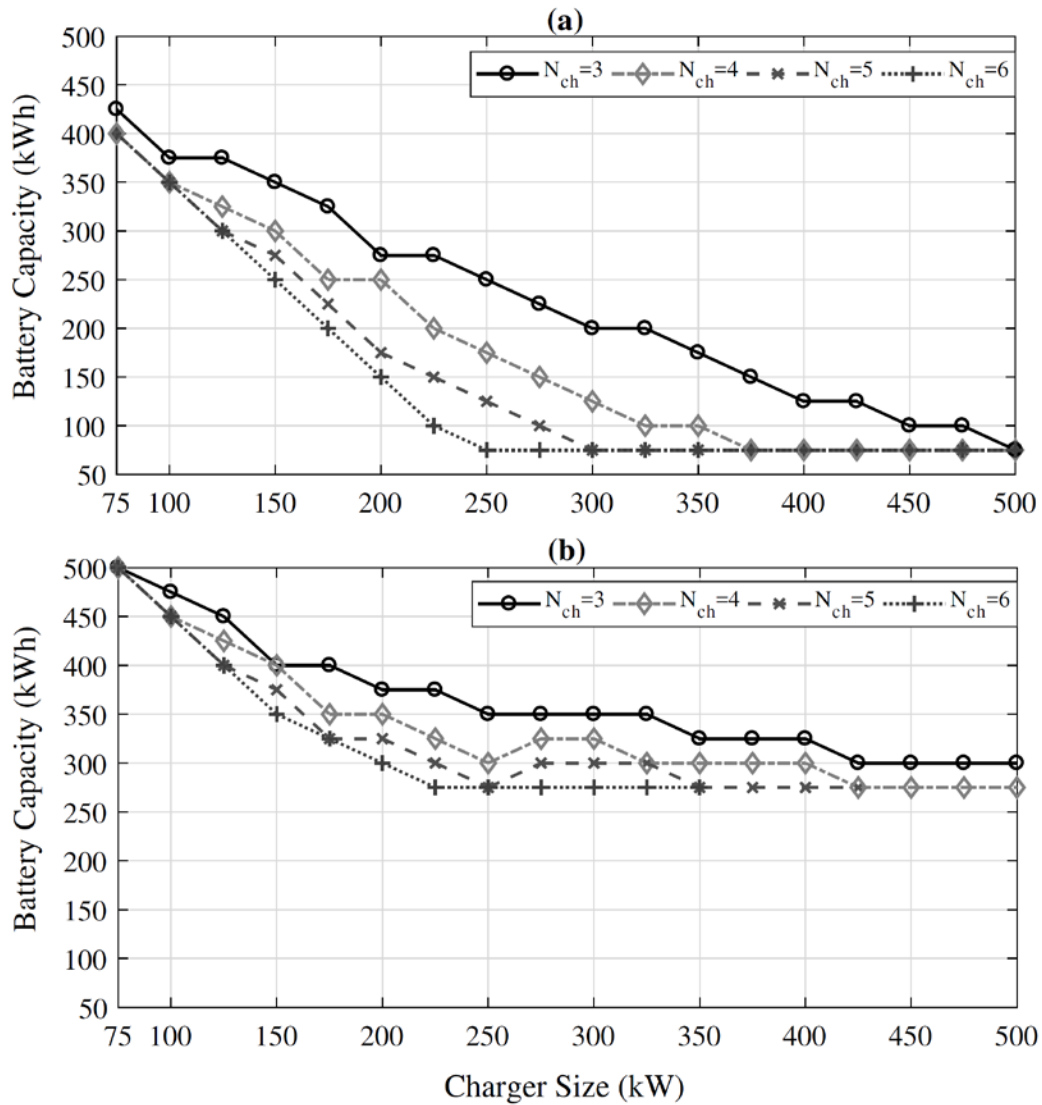


Figure 2.22 Feasible BEBs configurations at different number of chargers for; (a) Scenario 1, and (b) Scenario 2.

---

## 3. Multi-Regression Model Analysis

### 3.1 Introduction

Regression model analysis is the method of identifying and modeling the impact of a one or a set of variables on another variable of interest. A well-designed regression model employs the correlation between the variables to predict the value of the target variable(s). Generally, while designing a regression model, it is important to identify which factors matter most, as well as how these factors influence each other.

The value to be estimated is referred to as the dependent variable (or the target variable). On the other hand, the set of variables that are used to predict the value of the dependent variable is called the independent variables set (or the predictors). For example, using information such as the vehicle's horsepower and weight (predictors) to predict the fuel consumption in kilometers per liter (target variable). When the number of independent variables is two or more, the regression model is known as a multiple regression model.

The objective of this section is to build models to predict the expected minimum battery size needed to run a bus on a specific line using information about the existing bus schedule. These models can be utilized to provide an answer to the fundamental research question: *what size of electric bus battery is needed to replace existing diesel bus on a certain route.*

### 3.2 Regression Analysis Methods

The basic model of regression analysis is the linear regression which assumes that the relationship between the dependent and the independent variables is linear. Several extensions to this model have been developed based on assumptions related to input and output variables such as the simple linear regression, multi-regression and generalized linear regression.

Simple Linear Regression (SLR) models are based on one-to-one relationship between one dependent variable ( $x$ ) and only one independent variable ( $\hat{y}$ ). On the other hand, Multi-regression models extend the simple regression idea by allowing the model to have two or more independent variables as input ( $x_1, x_2, \dots, x_n$ ) and one dependent variable ( $\hat{y}$ ) in the output constructing many-to-one relationship as illustrated in *Figure 3.1*. Equations (3.1) and (3.2) describe linear regression models for the single-regression and multi-regression models, respectively.

$$\hat{y} = b_0 + b_1x \quad 3.1$$

$$\hat{y} = b_0 + b_1x_1 + b_2x_2 + \dots + b_nx_n \quad 3.2$$

In those equations, each of the coefficients of the regression model ( $b_i$ ) can be interpreted as the estimated change in ( $\hat{y}$ ) that corresponds to a one-unit change in the associated variable while the other variables are held constant.

Multi-regression models allow more information to be used for the dependent variable predictions, however they suffer from the following two key issues:

- Adding more independent variables does not mean that the regression will be better, i.e., produces better predictions; in fact, it can make the predictions worse which is known as “overfitting”. Hence in order to improve the performance of the predictor, the best independent variables should only be utilized in the model.
- Additionally, the independent variables are not only potentially related to the dependent variable but also, they may be correlated among each other. This issue is known as “multicollinearity”. Hence the ideal case is to have the independent variables only related to the dependent variable while being mutually independent.

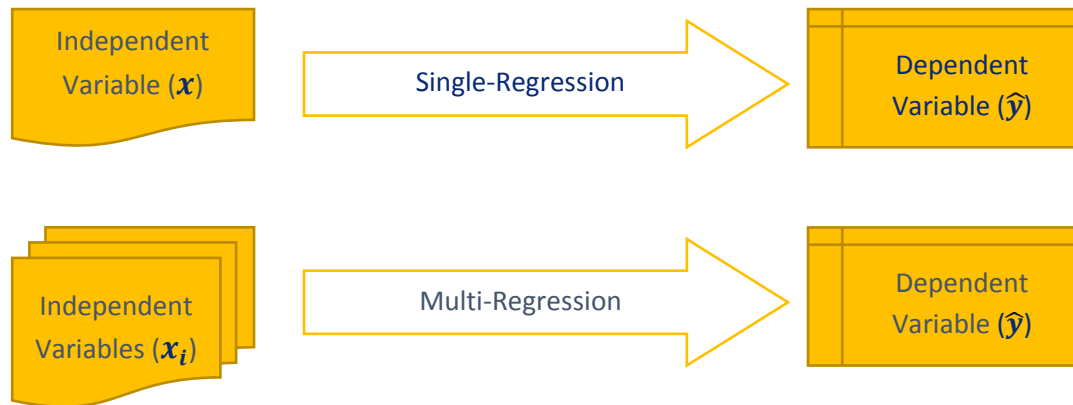


*Figure 3.1 Single versus Multi-Regression analysis models*

Generalized linear models (GLMs) allow the regression of response variables that do not have a normal distribution error via incorporation of a link function. Several types of statistical regression models fall under GLM such as logistic regression and Poisson regression. Recently, regression models have been fundamentally used by machine learning algorithms due to their simplicity and well-known properties.

Besides the selection of the model, the other important aspect of developing a regression model is performing the fitting which is the estimation of the parameters in the model. The most common fitting techniques used are Least-squares and Maximum-likelihood. The goal of fitting is to find the best fit model, i.e., find the values of the parameters (coefficients) that will minimize the prediction error. This error is defined as the difference between the input value and the predicted value using the model.

Finally, linear regression has been widely utilized in several fields such as biology, finance, economics, environmental and social sciences, and so many others. For example, in finance linear regression is used to quantifying the risk of an investment through finding the beta coefficient which relates the return on the investment in a stock to the return on overall market stocks.

### 3.3 Data Description

In order to estimate the battery size needed for the bus to replace an existing diesel bus while maintaining the same schedule, the information about the transit network is collected. The information includes data about each route and the battery size calculated for a different charger size. A sample of this information for few routes is shown in *Table 3.1*. The set of predictors include:

- Service hours (hour): the number of daily hours that the route is serviced by the assigned buses.
- Trip cycle time (minutes): the time in minutes required for one bus to complete one trip.
- Trip Frequency (minutes): the number of minutes between trips
- Recovery time (minutes): the time required for the bus to wait in the terminal before starting a new trip.
- No. of buses: number of buses assigned to service the route.
- Route (km): the length of the route in km
- No. Daily Trips: the total number of trips made on the routes by all the assigned buses.
- Battery size is also dependent on the charger size which can be in the range 100kW to 600kW

Finally, the target value, which is the battery size in kWh, can be between 100kWh to 900kWh.

The target value of each predictor is plotted with the target value to visually analyze the correlation relationship as depicted in Figure 3.2. From the figure, it can be noticed that routes with small numbers of operation hours scheduled, i.e. less than 10 hours, can run with lower battery capacity, i.e. less than 400kWh. Another interesting pattern that can be deduced is relevant to the recovery time. As shown in the figure, the lower the recovery time, the higher the battery capacity, with the reverse also being true.

*Table 3.1: Sample of transit network data for regression analysis*

Route name	Service hours (hour)	Trip cycle time (min)	Trip Freq. (min)	Recovery time (min)	No. of Buses	Route (km)	No. Daily Trips	Battery Size (kWh)	
								at: 150 kW Charger	at: 450 kW Charger
Dundas (Est)	22.9	56	5	8	5	21.7	95	675	100
Dundas (Wst)	21.9	56	5	8	5	20.5	97	625	100
Bloor (Est)	21.0	42	5	5	4	15.8	95	625	225
Bloor (Wst)	21.0	40	5	8	4	14.45	90	575	100
Sherway Gardens (Est)	17.5	40	20	5	3	18	48	625	350
Sherway Gardens (Wst)	17.6	47	20	4	3	19.5	48	600	575
Dixie (North)	21.4	50	10	4	4	19.2	85	650	650
Dixie (South)	20.5	52	10	4	4	19.2	83	600	575
Credit Woodlands (Est)	20.5	31	10	8	3	11.8	69	550	100
Credit Woodlands (Wst)	19.6	30	15	8	3	10.1	67	900	100

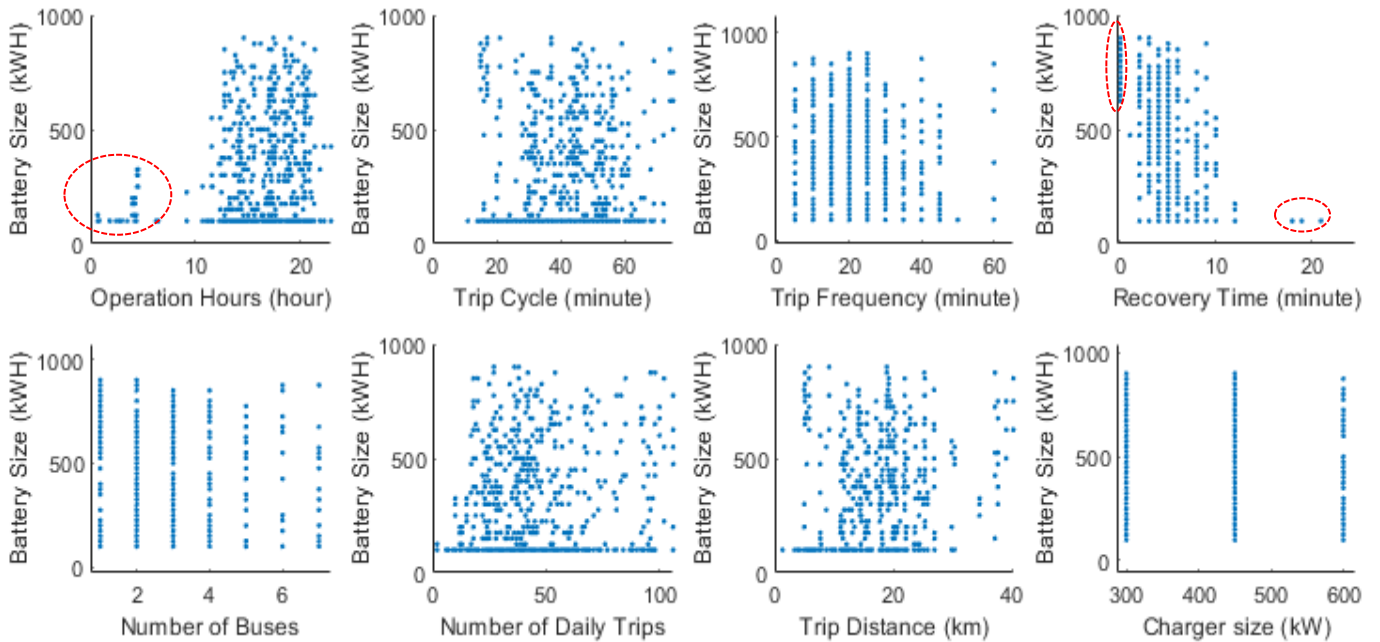


Figure 3.2: The correlation between the predictors and the target value (battery size)

### 3.4 Regression Model Selection

The main steps for training the regression model are shown in Figure 3.3. In the first step, the known input parameters are collected along with the known corresponding target value. Using the training data, the regression training is executed to generate the trained model. This model is then used to predict the unknown battery size for unseen input parameters as illustrated in Figure 3.4.

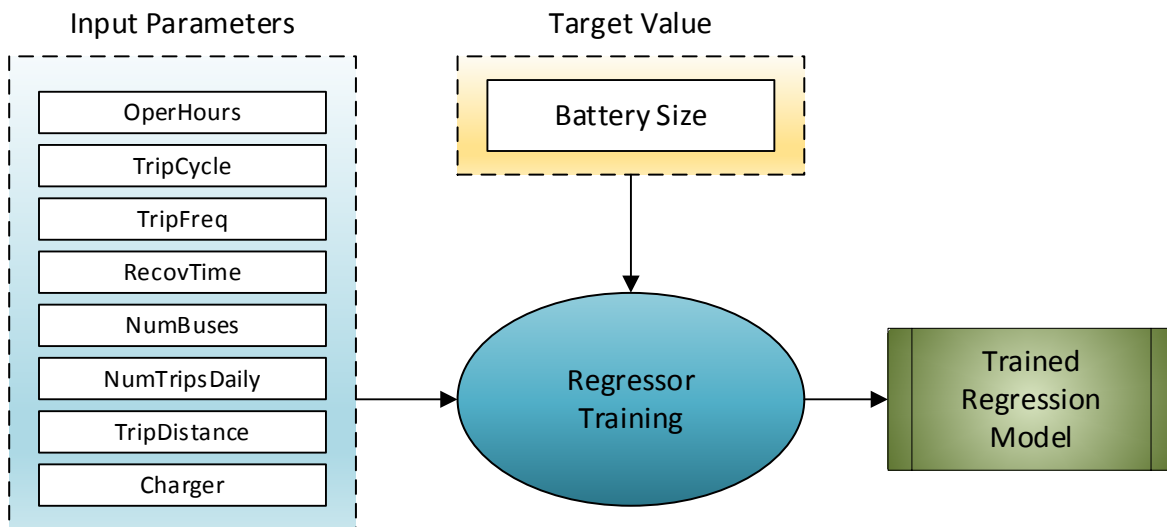


Figure 3.3: Regressor training process

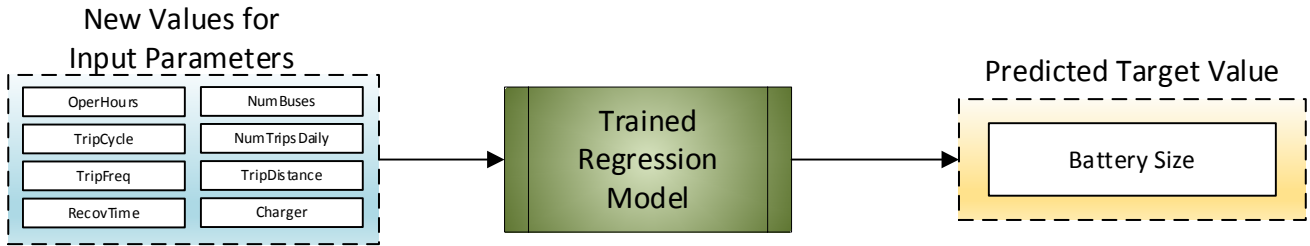


Figure 3.4: Making prediction using a trained regression model

In order to choose the best regression model, several types of regression models were trained and the total regression error was recorded. The model with the lowest error was found to be the Support Vector Machine (SVM) with Gaussian kernels. The root mean squared errors (RMSE) are reported in Table 3.2.

Table 3.2: The total error of several regression models

Model	Linear	Quadratic Polynomial	Cubic Polynomial	Gaussian
RMS Error (kWh)	179	120	92	44

### 3.5 Case Study 1: One Network with all Input Parameters

In this case study, the training data chosen is the route information, charger size and corresponding battery capacity of the Mississauga Transit network only. The model is trained using all the input parameters presented in Table 3.1 as the predicates without performing any preprocessing step for feature expansion and/or selection. The prediction results are shown in Figure 3.5. The individual predictions for a sample set of the routes of Mississauga Transit network are shown in Figure 3.6.

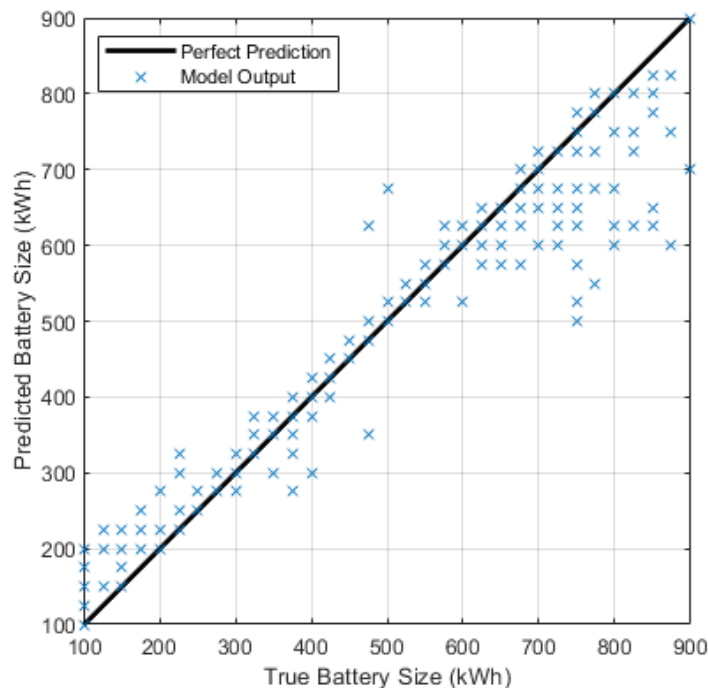


Figure 3.5: Predicted versus actual battery size

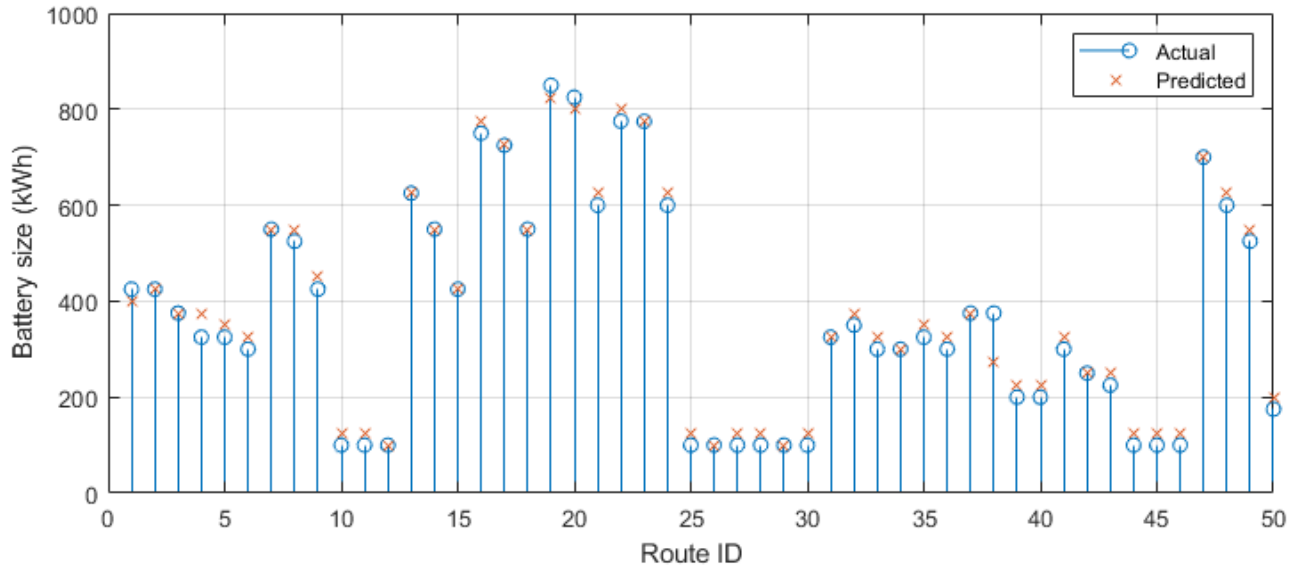


Figure 3.6: Sample of the predicted battery size for individual routes of Mississauga Transit Network

### 3.6 Case Study 2: Accuracy Enhancement

In addition to selecting a quality regression model, highlighting and quantifying the context-specific variables of input parameters of significant impact is also important. This process is known as feature selection and can be done by analyzing the dependencies between the target value and the features using statistical methods. Alternatively, when the number of items in the feature set are small, a manual selection can be done by removing some of the parameters, training the model using the remaining features, and then choosing the set of features that generates the model with the lowest error. Moreover, a feature extraction step is normally performed to reduce the number of input features by replacing a set of features with a new feature that may provide more useful information to the model than the individual features combined. Figure 3.7 shows the training of the regressor with feature expansion and selection preprocessing steps.

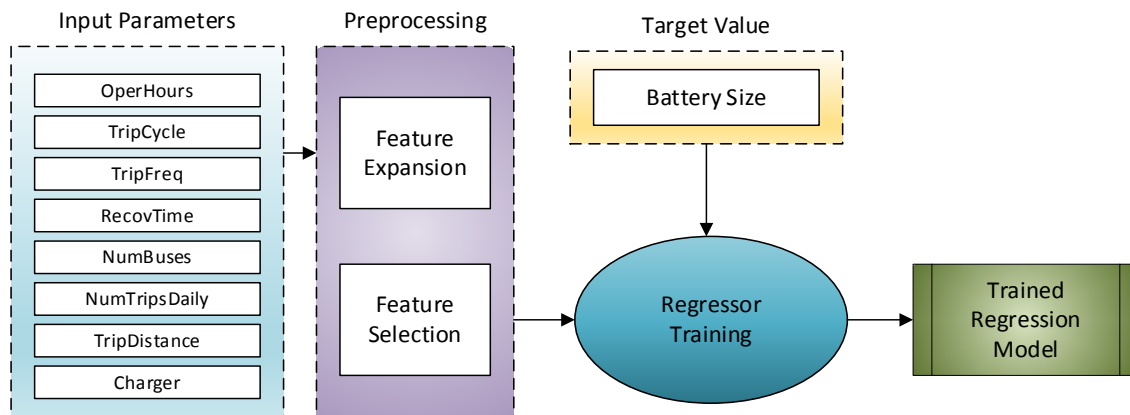
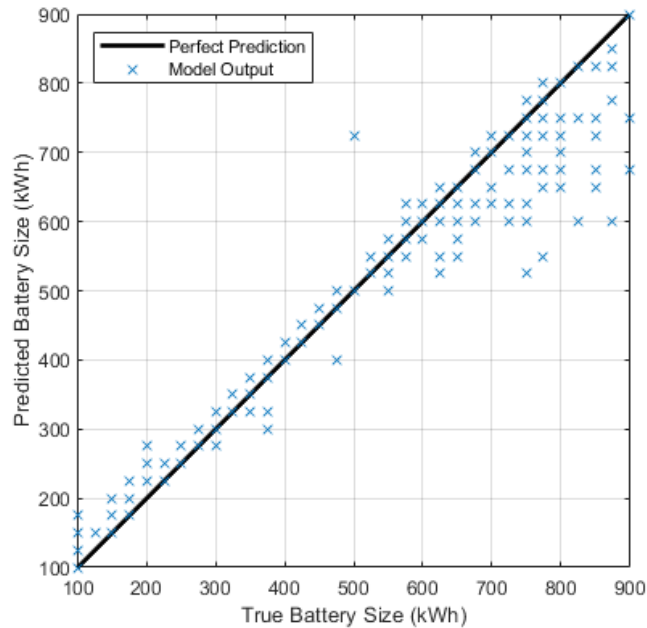
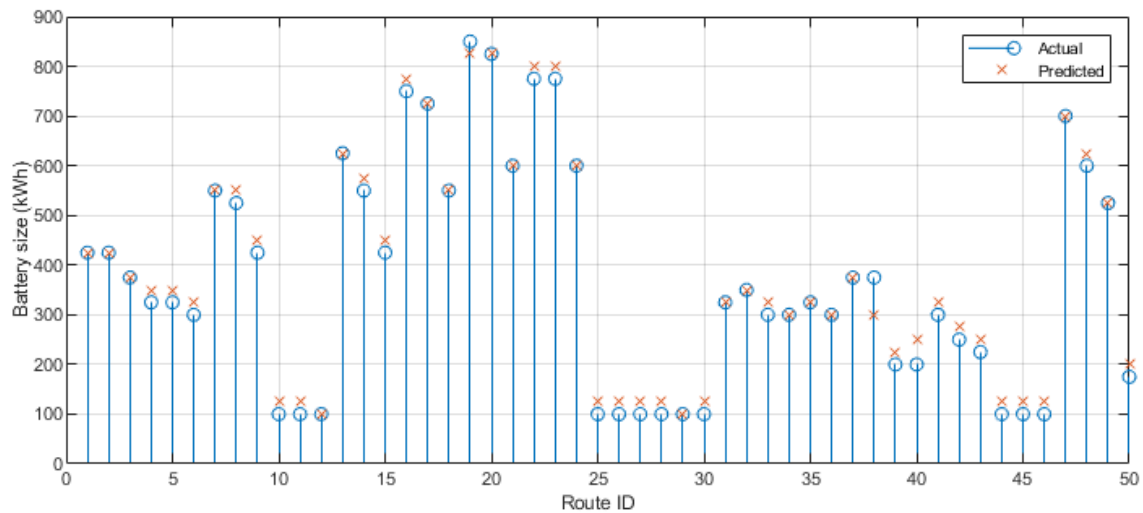


Figure 3.7: Regressor training with preprocessing of the features

In this case study, manual feature selection is performed, and statistical methods are applied to extract more useful features. During the manual selection, several different combinations of features were removed, and the regression model was retrained to reduce the error from 44 kWh to 42 kWh. Furthermore, independent component analysis (ICA) was applied to extract a new set of features that dropped the error to 41 kWh. Figure 3.8 and Figure 3.9 show the improved predictions.



**Figure 3.8: Predicted versus actual battery size (using the improved regression model)**



**Figure 3.9: Predicted battery size for individual routes of Mississauga Transit Network using improved regression model**

### 3.7 Case Study 3: Study with all networks to be trained

In the previous case studies, only the data of the Mississauga Transit Network was used to train and test the regression model. However, testing this model using data from only the Mississauga transit networks may increase the regression error due to using a small sample size of data. For example, as shown in Figure 3.10 by

the blue bars, the errors in predicting battery size for YRT and Brampton using Mississauga data are 191 kWh and 175 kWh, respectively. Therefore, in order to improve the prediction model, the data from all other transit networks, including YRT and Brampton, are used according to the process presented in the previous case study. As shown in Figure 3.9, the error in regression improves drastically, and is less than 50kWh (less than 15% error). This means that the regression model is more generalized and can be used to predict the battery size of other transit networks in the future.

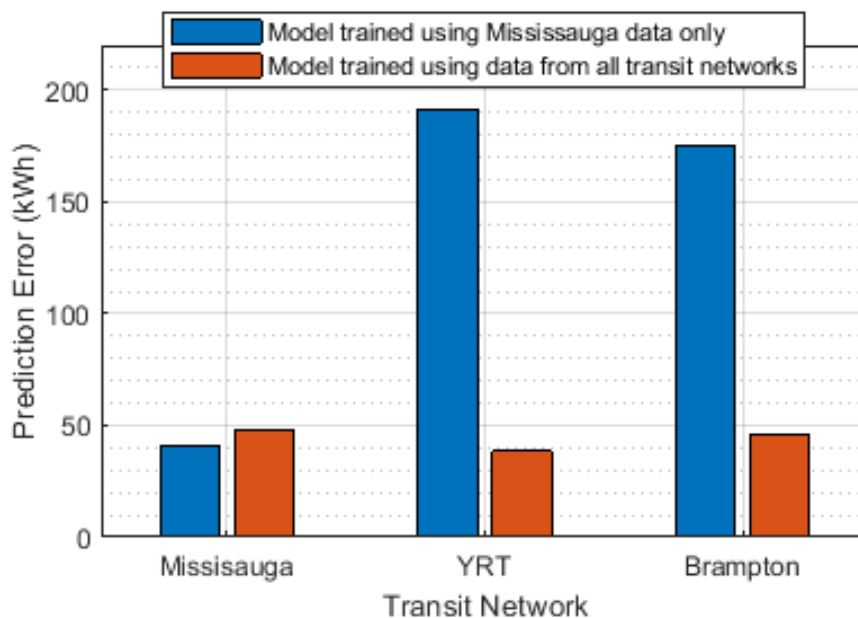


*Figure 3.10: The regression errors of the model developed using Mississauga data only*

## 4. Economic Cost and Environmental Impact Assessment

This section presents the quantification of economic costs and environmental benefits for the electrification of the studied transit networks. A comparative study is presented to cross compare the economic and environmental requirements of BEBs and Diesel buses (DBs). The following sub-sections present a brief description of the work process to evaluate the economic and environmental impacts.

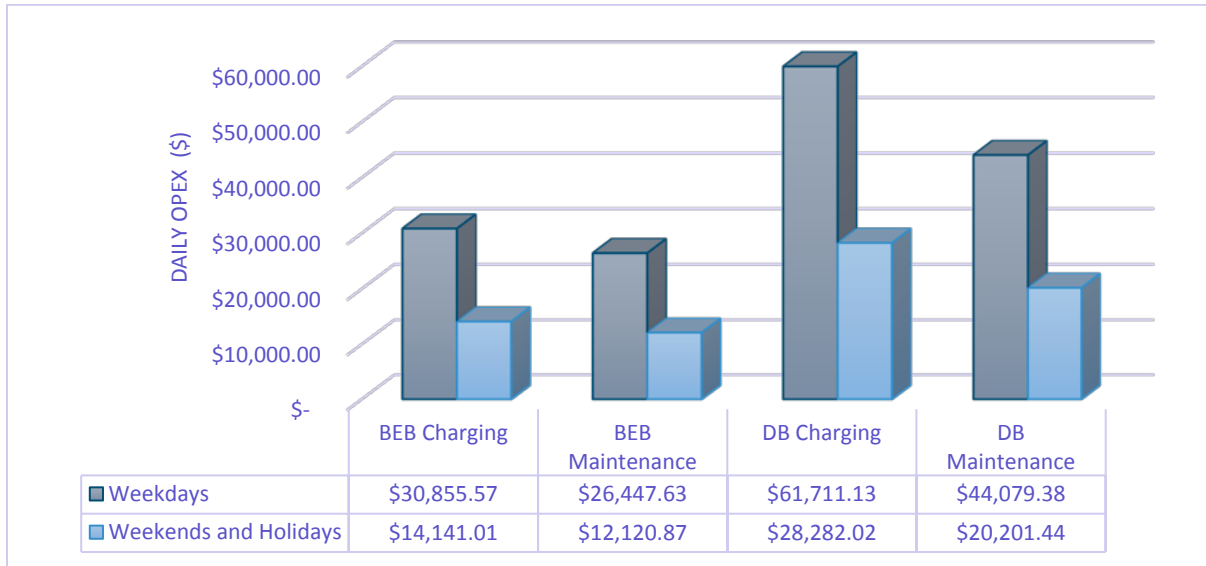
### 4.1 Economical Analysis

Table 4.1 presents the economic parameters that have been used to evaluate the annualized CAPEX and OPEX for BEBs and DBs. The OPEX consists of two components, which are charging/fueling costs for the BEBs/DBs, as well as their maintenance cost. Here, it is worth noting that the CAPEX of the BEBs is calculated as a function of their designed battery capacity, where a fixed price of \$525K is considered for the bus without the battery cost, while the battery cost rate is assumed to be 750 \$/kWh. Also, it is worth noting that an average charging cost of 0.175 \$/kWh is considered in this study, which is derived from the previous analysis presented in the technical report R3. The charging cost considers the Hourly Ontario electricity price, global adjustment, demand charge, and services cost. In order to maintain the annualized CAPEX and OPEX calculations, weekdays, weekends and holidays transit service schedules are considered in this study. Each of these service schedule results in a different covered distance, which, in turn, results in different patterns of charging profiles for the BEBs and different diesel fuel requirements for DBs. As such, the parameters shown in Table 4.1 are used to evaluate OPEX for weekdays, as well as weekends and holidays for both BEBs and DBs.

The results of the study for YRT buses are depicted in Figure 4.1, where the OPEX of weekends and holidays is almost half the OPEX of the weekdays. This is because the rider frequency is much less on the weekends and holidays as compared to the weekdays. Figure 4.2 presents the annualized CAPEX and OPEX for Brampton, Mississauga Transit (MiWay), and YRT. As shown in the figure, the OPEX of the BEBs is less than the DBs OPEX by 45%. In particular, BEBs' charging cost has 50% reduction as compared to diesel fuel cost, while BEBs maintenance cost has 40% reduction as compared to DBs. Such savings represents an annual savings of \$4.82M, \$5.69M, and \$3.6M for Brampton transit, MiWay, and YRT, respectively.

*Table 4.1 BEB and Diesel Bus Economic Parameters*

<b>Parameter</b>	<b>Value</b>
BEB Purchase Price (w/o battery cost)	525,000
Battery cost (\$/kWh)	750
BEB maintenance cost (\$/km)	0.3
BEB Charging Cost (\$/kWh)	0.175
Diesel BEB Purchase Cost (\$)	370,000
Diesel maintenance cost (\$/km)	0.5
Diesel Price (\$/L)	1.25
Diesel Consumption in L/km (\$)	0.56



**Figure 4.1 YRT Weekdays vs weekends Operation expenditure (OPEX)**

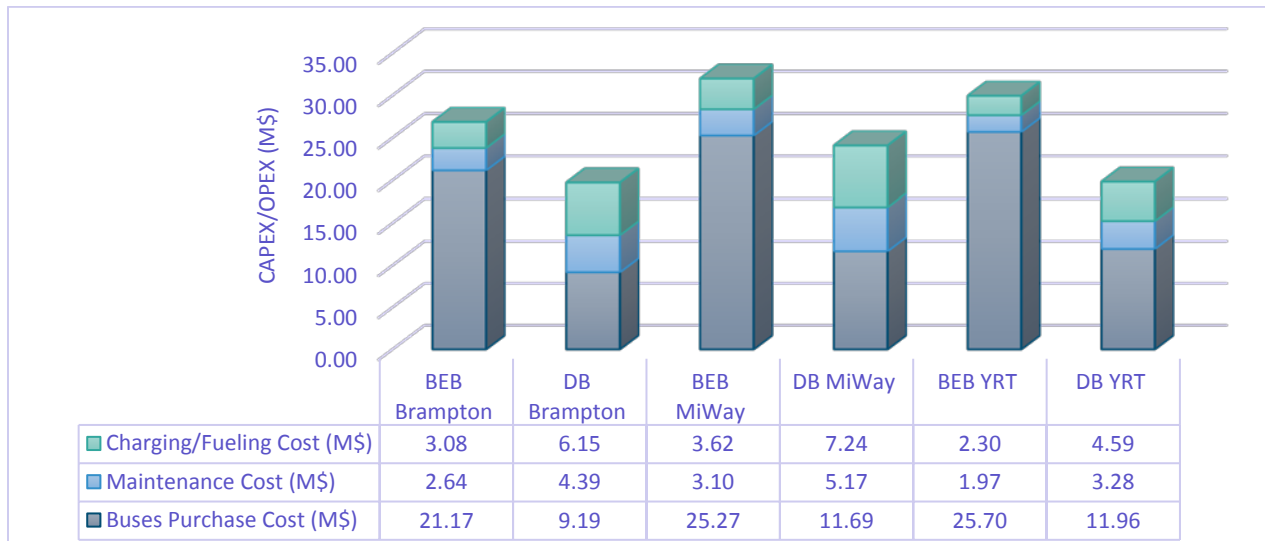


**Figure 4.2 Annualized BEBs vs DB Economic Analysis**

However, it should be noted that the CAPEX of the BEBs are more than two times higher than the DBs CAPEX. As shown in Table 4.2, the overall annualized CAPEX and OPEX of BEB transit electrification adds additional annual financial burden to the transit network operators by \$7.16M, \$7.89M, and \$10M for Brampton transit, MiWay, and YRT, respectively. This additional financial burden accounts for an increase of 36.3%, 32.7%, and 51% for Brampton transit, MiWay, and YRT, respectively. For this reason, further development, and enhancement in the BEBs technology is required to reduce the BEBs purchase cost to be competitive to the DBs.

*Table 4.2 Annual BEBs Economic Analysis*

<b>Transit Network</b>	<b>Brampton transit</b>	<b>MiWay</b>	<b>YRT</b>
<b>Annual OPEX saving</b>	\$4.82M	\$5.69M	\$3.6M
<b>Additional Annual Cost (CAPEX and OPEX)</b>	\$7.16M	\$7.89M	\$10M
<b>Annual Financial Increase</b>	36.3%	32.7%	51%

## 4.2 Environmental Analysis

BEB technology is expected to offer zero emission, quiet operation, and high reliability and efficiency. The assessment of the BEB GHG emission is usually carried out as a well-to-wheel assessment. This assessment is split into two phases: 1) well-to-tank emissions that indicate the GHG emissions during fuel production and distribution, and 2) tank-to-wheel emissions that indicate GHG emissions during energy utilization. The well-to-tank emission of renewable based electricity sources is generally represented as 20 gCo2eq/km. In this study, a standard non-renewable energy mix is assumed to have 720 gCo2eq/km, as is the accepted emission factor reported in the literature [4], [15]. This case study considers two scenarios for the GHG emission of BEBs analysis. The first scenario assumes that the BEBs will be supplied by an energy mix containing 100% renewable electricity, while the second scenario assumes a non-renewable electricity mix. To that end, Table 4.3 presents the well-to-wheel GHG parameters for BEBs and DBs.

Figure 4.3 shows the annual comparison among BEBs and DBs of CO<sub>2</sub> emissions for: (a) Brampton Transit, (b) MiWay, and (c) YRT. Each bar represents the amount of CO<sub>2</sub> equivalent emission in tones. As depicted in the figure, there is a 98.4% reduction in GHG emissions when the BEBs are charged from 100% renewable sources (compared to the GHG emissions of DBs). If the BEBs are charged using a non-renewable generation mix, a 41% emission reduction is achieved as compared to the GHG emissions produced by DBs.

*Table 4.3 BEB and Diesel Bus GHG Well-to-Wheel Emissions*

<b>Parameter</b>	<b>Value</b>
BEB Renewable Electricity GHG emission (gCo <sub>2</sub> eq/km)	20
BEB Electricity mix GHG emission (gCo <sub>2</sub> eq/km)	720
Diesel CO <sub>2</sub> emission (gCO <sub>2</sub> eq/km)	1222

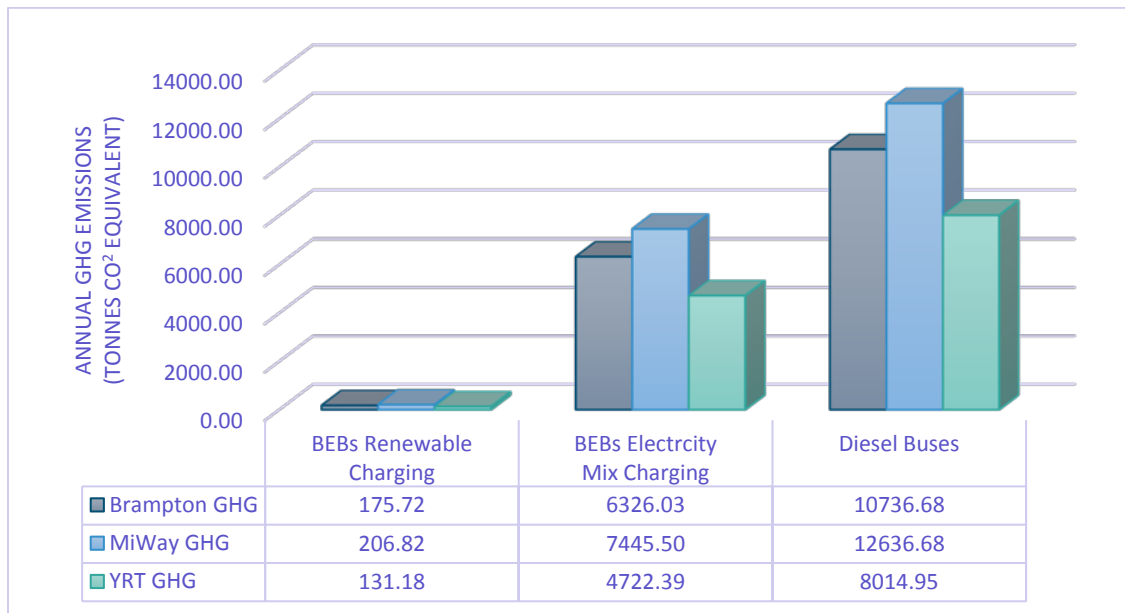


Figure 4.3 BEBs vs DB Environmental Impact

## 4.3 Province Level Economic and Environmental Analysis

Table 4.4 presents the annual covered distance in Ontario by school buses, city public buses and the GO bus (intercity transit network), in addition to their estimated annual energy consumption with an average energy consumption rate of 2 kWh/km for all electric buses. Using the operation and maintenance cost parameters given in Table 4.1, Table 4.5 shows a comparison between the operation and maintenance costs of both BEB-based and diesel-based transit networks. As depicted in the table, the province of Ontario has a potential to save about \$300M and \$170M annually for the transit networks operation and maintenance cost, respectively, due to the electrification of its bus fleets.

Table 4.4 Ontario's Transit Bus Networks Aggregated Distance and Energy Consumption According to IESO Zones

IESO zone	School Buses		City Public Transit Buses		Go Bus		Total (GWh/year)
	Annual kms	GWh/year	Annual kms	GWh/year	Annual kms	GWh/year	
West	35.97	71.92	19.27	38.55	0	0.00	110.47
Southwest	48.2	96.35	45	90.08	11.881	23.75	210.18
Bruce	8	16.03	0	0.00	0	0.00	16.03
Niagara	19.4	38.83	8.812	17.63	5.94	11.88	68.34
Toronto	59.94	119.88	340.3	680.65	35.63	71.26	871.79
Essa	22.58	45.16	4.87	9.74	0	0.00	54.90
East	47.11	94.22	10	20.02	0	0.00	114.24
Ottawa	25.56	51.12	63	126.25	0	0.00	177.37
Northeast	27	54.02	9.2	18.40	0	0.00	72.42
Northwest	6.72	13.43	3.3	6.60	0	0.00	20.03
<b>Total</b>	<b>300.5</b>	<b>600.97</b>	<b>504</b>	<b>1007.92</b>	<b>53.441546</b>	<b>106.88</b>	<b>1715.77</b>

Table 4.6 provides a comparison for the contribution of GHG emission between electrified and diesel-based transit networks in the province of Ontario. As depicted in the table, Ontario has the potential to save 430,658 tCO<sub>2</sub>-eq. annually if BEBs are supplied from a non-renewable electricity mix. When BEBs are supplied from 100% renewable electricity, a reduction of 1,031,178 658 tCO<sub>2</sub>-eq. could be achieved.

*Table 4.5 Ontario Aggregated Operation and Maintenance Cost Comparison BEB vs. Diesel Bus according to IESO Zones*

	Battery Electric Bus		Diesel Bus	
	Charging Cost (M\$)	Maintenance Cost (M\$)	Diesel Fuel Cost (M\$)	Maintenance Cost (M\$)
<b>School Buses</b>	105.2	90.2	210.4	150.2
<b>City Public Transit Buses</b>	176.4	151.2	352.8	251.98
<b>Go Bus</b>	18.7	16	37.41	26.72
<b>Total</b>	300.3	257.4	600.61	428.9
<b>Reduction %</b>	<b>50%</b>	<b>60%</b>	-	-

*Table 4.6 Ontario Aggregated GHG Emission Comparison BEB vs. Diesel Bus according to IESO Zones*

	Renewable Emissions (tCO <sub>2</sub> -eq.)	Electricity-mix Emissions (tCO <sub>2</sub> -eq.)	Diesel Emissions (tCO <sub>2</sub> -eq.)
<b>School Buses</b>	6009.7	216348.8	367191.94
<b>City Public Transit Buses</b>	10079.2	362851.1	615838.98
<b>Go Bus</b>	1068.83	38477.9	65305.57
<b>Total</b>	17157.73	617677.8	1048336.49

---

## 5. Development of an Interactive Graphical User Interface

This section introduces an interactive **Web-based Electric Bus Simulation Toolbox (WEBST)** that has been developed in this project to analyze electrified transit bus systems. WEBST is comprised of three interdependent modules: Energy Consumption, Charging Scheduling, and Economic and Environment Analysis. In particular, given the technical specification of BEBs, the transit system block data i.e., trips scheduling, and the speed profile of each scheduled trip, WEBST is capable of: (i) generating the BEB energy consumption profile in each scheduled trip, (ii) facilitating a comparison of the results of energy consumption with the data claimed in the BEB manufacturer datasheet, (iii) evaluating the feasibility of a user-specified BEB and charging configuration to satisfy the fleet operation requirements, (iv) generating the opportunity and/or overnight charging schedules for each BEB, and (iv) performing economic and environmental analysis using user-supplied parameters. The toolbox is built using web-based technologies, meaning that it can be run on existing infrastructure and does not require external software packages to be installed by the end-user. It has user-friendly interfaces with ease of access across multiple platforms and locations. The toolbox is intuitive in terms of producing simulation analysis results that can be comprehended by non-technical users. The availability of such an online toolbox can be used to benchmark the energy consumption efficiency of BEB models reported by manufactures and test the operation feasibility and technical performance of BEB fleets.

### 5.1 Data Entry and Inspection Interfaces

In general, the toolbox interface consists of three main panels: (1) a navigation panel that allows the user to choose one of the toolbox's modules to interact with; (2) input/action panel, which allows the user to input the information related to the selected module and perform an action (e.g. generate speed profile); and (3) output panel, where the results of the evaluation/actions are shown to the user.

Under the category of input data, WEBST offers several interfaces for entering BEB data, as shown in the screenshot in Figure 5.1. The WEBST toolbox offers some standard models of BEBs for the user to select, or the user may enter customized data and save it as a new bus model that can be used later in the studies.

With regards to routes data, WEBST toolbox allows the user to visualize bus routes on the map and query information about the route selected as shown in Figure 5.2. The user can also plot the elevation profile of the route along the traveled distance. The elevation data is used for calculating more accurate BEB energy consumption per traveled distance. A sample elevation profile is depicted in Figure 5.3.

The study of a complete transit network electrification requires details about the transit network blocks. WEBST toolbox provides an interface for entering the block data table as illustrated in Figure 5.4. The user can add, modify, or delete any row from the table, in addition to the ability of importing the data from an external data file. The user can also filter the available blocks based on the transport company and edit the block details via the buttons provided in the action column

Bus Data

Route Data

Speed Profile

---

Energy Consumption

Charging Scheduling

---

About

### New Flyer

Battery capacity: 545 kWh  
Seats: 40 passengers

Select

### BYD K11

Battery capacity: 652 kWh  
Seats: 45 passengers

Select

### BYD Double Decker Coach

Battery capacity: 496 kWh  
Seats: 78 passengers

Select

Enter bus specifications (Current bus: New Flyer)

Electric Bus Mass (Kg) <input style="width: 90%;" type="text" value="13835"/>	Rolling Resistance Coefficient <input style="width: 90%;" type="text" value="0.015"/>	Bus Facing Area m <sup>2</sup> <input style="width: 90%;" type="text" value="8.58"/>
Inverter Efficiency <input style="width: 90%;" type="text" value="0.95"/>	Electric Motor Efficiency <input style="width: 90%;" type="text" value="0.85"/>	Driver Shaft Efficiency <input style="width: 90%;" type="text" value="0.95"/>
Auxiliary Load for Electric Bus (KW) <input style="width: 90%;" type="text" value="0"/>	Drag Coefficient <input style="width: 90%;" type="text" value="0.65"/>	Air Density <input style="width: 90%;" type="text" value="1.2258"/>
Gravity (m/s <sup>2</sup> ) <input style="width: 90%;" type="text" value="9.8"/>	<input style="width: 50px;" type="button" value="Save"/>	

**Figure 5.1 The main screen to enter electric bus specifications**

### Select route

Route: Brampton Transit Route 17

Route start: Bramelea Terminal

Route end: Trinity Common Terminal

Total distance: 5 km

Generate Route Elevation Plot

The map displays a blue route line connecting Bramalea Terminal (18/18B-NB Departure) and Trinity Common Terminal (5/5A EB/505). A callout box indicates a travel time of 26 minutes with buses every 12 minutes. Another callout shows 18 minutes every 20 minutes. The map includes street names like South New Blvd and 410, and landmarks like Chinguacous Park.

**Figure 5.2 Visualize bus routes and query information about the route**

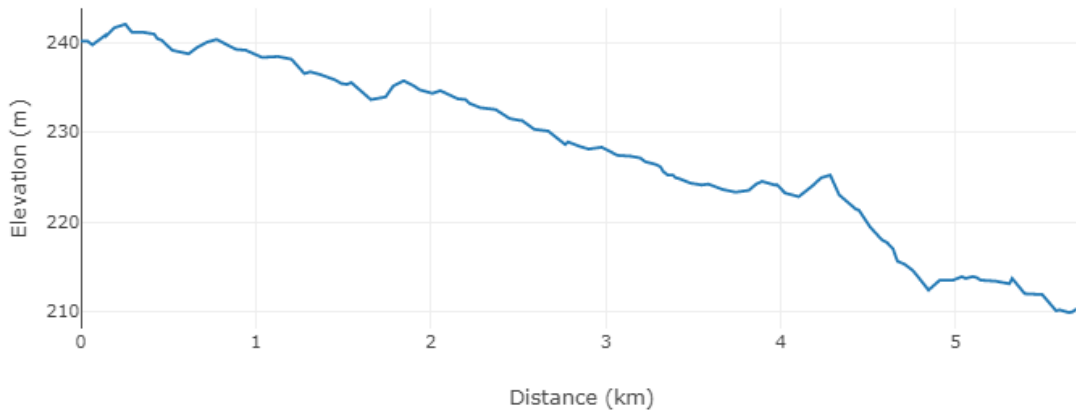


Figure 5.3 Elevation profile of bus route shown per the distance

## Block Details

+ Add New Block

All
  Barrie
  Bradford
  Brampton
  Hamilton
  Midland and Penetanguishene
  Mississauga
  St. Catharines
  YRT

Transport Agency	Route #	Route name	Start point	End point	Day of week	Start time	End time	Trip cycle time (min)	Recovery time (min)	No. of complete daily trips	No. of partial daily trips	No. of stops	Route distance (km)	Actions
YRT	1	Eastbound to Box Grove Walr...	1	2	WD	4:00 AM	1:22 AM	55	5	31	3	10	22.8	
YRT	1	Eastbound to Box Grove Walmart	1	2	Sat	6:10 AM	1:18 AM	51	5	24	2	10	22.8	
YRT	1	Eastbound to Box Grove Walmart	1	2	Sun	7:39 AM	11:22 PM	50	5	17	1	10	22.8	
YRT	1	Westbound to Richmond Hill Ce...	2	1	WD	4:30 AM	12:35 AM	52	5	31	1	8	23.2	
YRT	1	Westbound to Richmond Hill Ce...	2	1	Sat	6:20 AM	1:17 AM	52	5	24	1	8	23.2	
YRT	1	Westbound to Richmond Hill Ce...	2	1	Sun	7:52 AM	11:24 PM	45	5	17	1	8	23.2	
YRT	2	Eastbound to Markham Rd.	3	2	WD	5:14 AM	11:29 PM	46	5	36	2	9	18.4	
YRT	2	Eastbound to Box Grove Walmart	3	2	Sat	8:00 AM	11:57 PM	58	5	29	0	9	25.7	
YRT	2	Eastbound to Box Grove Walmart	3	2	Sun	8:45 AM	11:16 PM	60	5	14	0	9	25.7	
YRT	2	Westbound to Finch GO Bus Ter...	2	3	WD	5:19 AM	12:18 AM	56	5	40	4	9	22.11	
YRT	2	Westbound to Finch GO Bus Ter...	2	3	Sat	8:00 AM	11:56 PM	63	5	29	0	9	27.4	
YRT	2	Westbound to Finch GO Bus Ter...	2	3	Sun	8:44 AM	11:15 PM	56	5	14	0	9	27.4	
YRT	3	Eastbound to Steeles Ave. & Do...	4	5	WD	4:56 AM	11:04 PM	66	5	31	3	7	23.93	
YRT	3	Eastbound to Steeles Ave. & Do...	4	5	Sat	8:45 AM	9:27 PM	58	5	19	1	7	23.93	

Figure 5.4 A screenshot of block details table

The energy consumption of the BEB is the first WEBST module that is evaluated using Newton’s second law of motion, which consists of four force terms: inertia, gravity, rolling resistance, and the aerodynamic force. This energy efficiency calculation model was validated using the ADVISOR simulation tool that produced values matching the results of the WEBST model. The WEBST toolbox offers the privilege of generating high-resolution quasi-speed profiles for the users to conduct their studies. The quasi-speed profile is generated according to a developed controlled-random speed profile function, where the user inputs the maximum and minimum route speed limits, BEB maximum acceleration, and the duration of both ramping up (initial acceleration) at the beginning of the trip and ramping down (deceleration) at the end of the trip. On the other hand, WEBST toolbox provides the option to upload a specific speed profile data file and store it in the cloud. An illustrative screenshot of the speed profile generation is shown in Figure 5.5.

WEBST calculates the energy consumption using the generated or entered/uploaded speed profile, the BEB specifications, and the route information. The results are plotted in Figure 5.6 showing a screenshot of the energy consumption profile and the power tractions of a simulated BEB at each time step of the simulation.

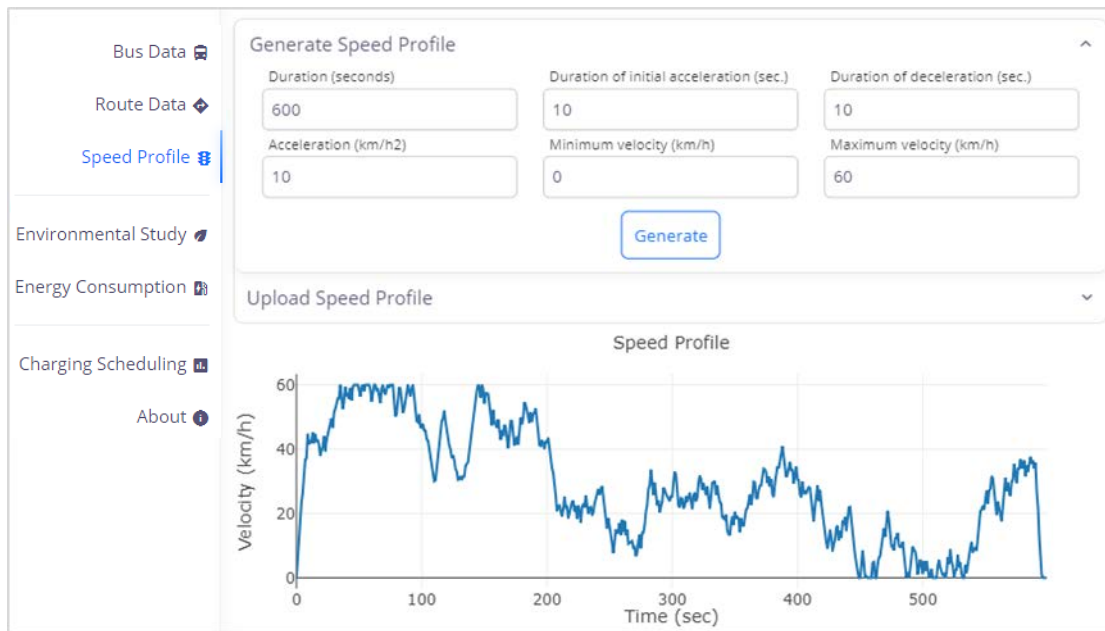


**Figure 5.5** A snapshot of the speed profile generation in the WEBST toolbox

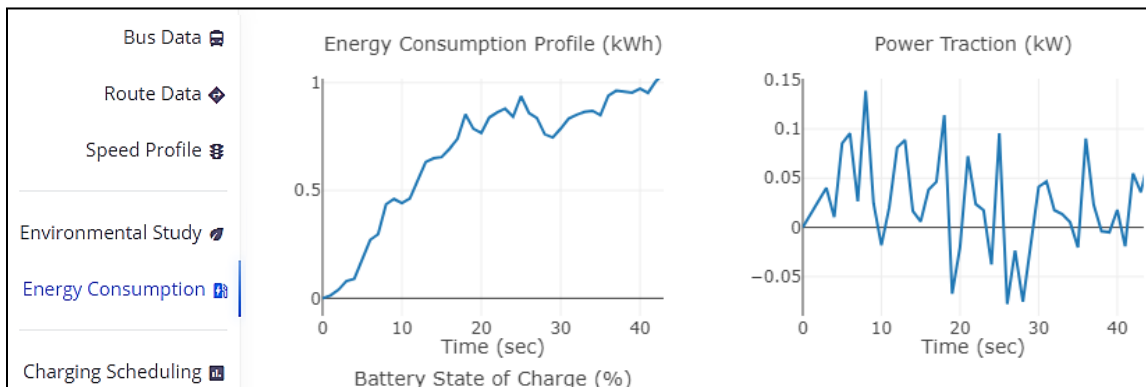


**Figure 5.6** A screenshot of energy consumption analysis output

The second module aims to allocate the charging schedules of each BEB in the transit network. In this regard, WEBST enables the user to insert the data of the operational electrified route in forms of operational blocks (i.e., set of consecutive trips performed by the same BEB). As shown in Figure 5.4 each operational block is defined by a starting time of the first trip, end time of the last trip, recovery/layover time in minutes (i.e., opportunity time to recharge the battery), and route distance in km. Here, it is worth noting that WEBST allows the user to either use the energy consumption of the BEB that is calculated in the first stage or to re-enter another value. Using the block information, WEBST calculates the arrival SOC,  $SoC_{bj}^{Arr}$ , of BEB  $b$  on a given route after a trip  $j$ . Then, after its arrival, the BEB will have the opportunity to recharge its battery within the recovery time. In consequence, the departure SOC of the BEB,  $SoC_{bj+1}^{Dep}$ , for trip  $j+1$ , after recharging the BEB battery is calculated. Afterwards, WEBST recursively calculates the BEB SOC performance after delivering the given transit service, in addition to reporting the BEB charging profile across the day. Detailed data of transport network agency blocks can be entered from the *Route Data* screen as shown in Figure 5.4.

## 5.2 Electric Power Utility and Optimization Setup Interfaces

WEBST provides the user with interfaces to model the electric power distribution network using the standard nodes/lines model representation. As such, the user can upload a data file of the power systems nodes and modify or add additional nodes using the nodes data interface shown in Figure 5.7. A similar interface for lines data is shown in Figure 5.8.

Electrical Feeder Nodes Data

Nodes data: 
Upload Data
+ Add New Node

bus_id	type	Vm	Va	Pd	Qd	Pg	Qg	Qg_min	Qg_max	Pg_min	Pg_max	Psh	Qsh	Actions
1	1	1.05	0	0	0	8	0	-20	20	0	0	0	0	
2	3	1	0	0.1	0.06	0	0	0	0	0	0	0	0	
3	3	1	0	0.09	0.04	0	0	0	0	0	0	0	0	
4	3	1	0	0.12	0.08	0	0	0	0	0	0	0	0	
5	3	1	0	0.06	0.03	0	0	0	0	0	0	0	0	
6	3	1	0	0.06	0.02	0	0	0	0	0	0	0	0	
7	3	1	0	0.2	0.1	0	0	0	0	0	0	0	0	
8	3	1	0	0.2	0.1	0	0	0	0	0	0	0	0	
9	3	1	0	0.06	0.02	0	0	0	0	0	0	0	0	
10	3	1	0	0.06	0.02	0	0	0	0	0	0	0	0	
11	3	1	0	0.045	0.03	0	0	0	0	0	0	0	0	
12	3	1	0	0.06	0.035	0	0	0	0	0	0	0	0	

Figure 5.7 WEBST interface for entering electric power distribution nodes data

## Electrical Network Data

Lines data:

 Upload Data

 Add New Line

From Node	To Node	R (Ohm)	X (Ohm)	B (Ohm)	Transformer Ratio	Line Rating (MW)	Actions
1	2	0.000574	0.000293	0	1	0	 
2	3	0.00307	0.001564	0	1	0	 
3	4	0.002279	0.001161	0	1	0	 
4	5	0.002373	0.001209	0	1	0	 
5	6	0.0051	0.004402	0	1	0	 
6	7	0.001166	0.003853	0	1	0	 
7	8	0.00443	0.001464	0	1	0	 
8	9	0.006413	0.004608	0	1	0	 
9	10	0.006501	0.004608	0	1	0	 
10	11	0.001224	0.000405	0	1	0	 
11	12	0.002331	0.000771	0	1	0	 

*Figure 5.8 WEBST interface for entering electric power distribution lines data*

The constraints and parameters of the study are shown in Figure 5.9. The user can choose from a list of multiple objectives under the **Objective Function** group of options. Additionally, parameters for the cost of charger installation as dollar per kW, the cost of the battery per kWh, and the cost of charger can be entered. In the next group for **Transit Constraints**, the user can set the desired range of battery capacity, the range of charger rating, the desired level of the battery state of charge to maintain during the bus's trips, as well as the number of chargers allowed to operate simultaneously on one charging station. Next, the user has the option to set some constraints to the power system network. Finally, advanced options for whether to consider an energy storage or not can be chosen for the optimization algorithm.

### Optimization Study Constraints and Parameters

**Objective Function:**

- Minimize Total Cost of Ownership
- Minimize Total Greenhouse Gas Emission
- Maximize the electrification integration (100% transit electrification)

Charger Installation Cost (\$/kW): - 450 +

Battery Cost (\$/kWh): - 750 +

Charger Cost (\$/charger): - 100000 +

---

**Transit Constraints:**

Battery Capacity (kWh) Min: 100 Max: 900

Charger Rating (kW) Min: 150 Max: 600

BEB State of Charge (SoC) Min: 20 Max: 90

No. of Simultaneous Chargers Min: 1 Max: 6

---

**Power System Constraints:**

Node's voltage magnitude (%) Min: 95 Max: 105

Power Factor (%) Min: 95 Max: 100

Max. Substation Transformer Capacity (%) - 85 +

Max. Feeder's Power Loading (%) - 85 +

Max. drawn power by a charging station (kW) - 2000 +

---

**Other Options:**

- Energy Storage Integration for cost minimization
- Energy Storage Integration to reduce charging intermittancy

**Figure 5.9** Interface for setting the optimization parameters and constraints

## 5.3 Economic and Environmental Analysis Interfaces

This module allows the user to conduct studies on the economic and environmental impact of replacing existing diesel buses with battery electric buses. The module requires some parameter inputs concerning the electric buses such as the base cost of the bus excluding the battery, the cost of a battery unit (per kWh), estimated average maintenance cost of the electric bus (per km), and the electricity price for charging the battery (\$/kWh). On the other hand, similar parameters for diesel buses are used to calculate CAPEX and OPEX for selected transport companies from the results obtained via the second module. Moreover, the environmental study includes the estimated GHG emissions from operating battery electric bus (BEB) and diesel bus (DB) on the selected transport network fleet using CO<sub>2</sub> equivalent emission rates for electricity generation and diesel consumption. Lastly, the toolbox has default values for the various parameters and allows the user to utilize some other rates which are reflected within the analysis after clicking the update button.

Under the Environmental Study module, the user can enter the study parameters as shown in Figure 5.10. The parameters are organized under two categories for battery electric buses (BEBs) and diesel buses (DB). Then, the user chooses which networks are to be included in the results and clicks the update button to reflect the changes in the results as shown in Figure 5.11 and Figure 5.12.

The screenshot shows a web-based interface for entering study parameters. On the left is a navigation menu with options: Bus Data, Route Data, Speed Profile, Environmental Study (highlighted), Energy Consumption, Charging Scheduling, and About. The main content area is titled 'Economical and Environmental Study Parameters' and is organized into two sections:

- Battery Electric Bus (BEB):**
  - Bus Price (\$CAD) excluding battery: 525000
  - Maintenance cost (\$/km): 0.3
  - Battery unit cost (\$/kWh): 750
  - Charging Cost (\$/kWh): 0.175
  - Renewable Electricity GHG emission (gCo2eq/kWh): 20
  - Electricity mix GHG emission (gCo2eq/kWh): 720
- Diesel Bus (DB):**
  - Bus Price (\$CAD): 370000
  - Maintenance cost (\$/km): 0.5
  - Fuel price (\$/L): 1.25
  - Fuel Consumption (L/km): 0.56
  - Diesel CO<sub>2</sub> emission (gCo<sub>2</sub>eq/km): 1222

Below these sections is a 'Transport Agency:' section with checkboxes for: All, Barrie, Bradford, Brampton (checked), Hamilton, Midland and Penetanguishene, MIWay (checked), St. Catharines, and YRT (checked). An 'Update' button is located at the bottom right of the parameter input area.

Figure 5.10 A screenshot of parameter input screen for the economic and environmental study

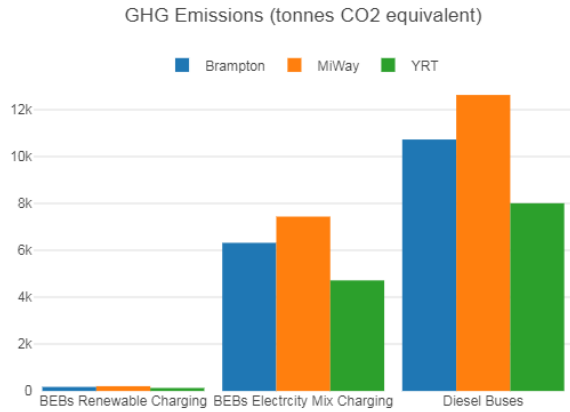


**Figure 5.11** Sample result for the GHG emissions of three transport networks

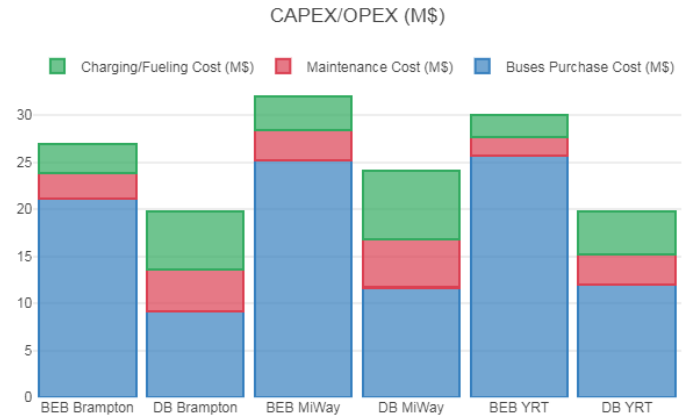


**Figure 5.12** Sample result for the CAPEX/OPEX of three transport networks

---

## 6. CONCLUSIONS

This work has contributed to the development of a modeling and simulation toolbox that allows the analysis of the power flow at grid-scale for inclusion of charger loads at desired BEB operating schedules. The modelling tools include Microsoft® Access & Excel, MATLAB® scripting and CYMEDIST software. These tools successfully simulated and analyzed various possible conditions at grid-scale within the province of Ontario. The modelling and simulation from this work resulted in the design of a utility-transit model for the BEB configuration design. Further, regression, economical, and environmental analysis were carried out to better understand the BEB design requirements and cost analysis for opportunity and overnight charging scenarios, as well as the assessment of charger impacts on the system.

The key findings and conclusions of this work are presented below:

1. At heavy power loading conditions, power distribution systems may not be able to satisfy the charging requirements of the BEB fleet when the BEBs configuration and charging schedule are not optimally designed. This was seen in the Belleville case study in Section 2.3.2, where opportunity charging caused undervoltage violations within the benchmark PDS.
2. In general, when a PDS is facing high level of congestion under a certain BEB configuration, the following design aspects related to the BEB system can be considered:
  - Increase the BEBs' battery capacity to deliver few consecutive trips without the need for a charging session
  - Adjust the charging schedule so a smaller number of BEBs could have the opportunity to charge during heavy-loading conditions
  - Decrease the charger's size to allow BEBs to be charged without impacting the PDS during heavy-loading conditions
  - Increase the number of chargers to sufficiently charge the BEBs before and after the heavy-loading conditions given that BEBs will not have the full opportunity to charge during such conditions.
3. BEBs chargers will cause consistent increase in electric demand during all hours of the day. As seen in the analysis of Feeder 12M3 of Alectra's service territory (Section 2.3.1), the expected increase in the peak demand ranges from 11% to 22% using a 300kW charger and from 10% to 30% using 600kW charger.
4. The voltage in Alectra's PDS within the Vaughan area is unlikely to be impacted after the electrification of transit network due to reserve feeder capacity and the operation of voltage regulators.
5. Buttonville substation utilization rate will increase from 39% to 41.4% considering average demand, and from 76.5% to 83.5% based on the peak demand.
6. Fast response energy storage system might be needed to eliminate the high intermittency of the electrified transit network charging profile. In such a case, a super capacitor ESS that is characterized by fast response can eliminate such intermittency.
7. Compared to the fuel OPEX of DBs, the charging OPEX of BEBs is 50% less. BEBs also provide a maintenance cost reduction of 40% as compared to BEBs.
8. BEB transit electrification increases the annualized cost (CAPEX and OPEX combined) between 32% to 50% for YRT, Brampton, and Mississauga transit networks.

- 
9. BEBs will provide a 98.4% reduction in GHG emissions as compared to DBs if the BEBs are charged by 100% renewable electricity. This translates to annual GHG savings of 1,031,178 tCo<sub>2</sub>-eq. for Ontario.
  10. BEBs will provide a 41% reduction in GHG emissions as compared to DBs if the BEBs are charged by a standard, non-renewable electricity mix. This translates to annual GHG savings of 430,658 tCo<sub>2</sub>-eq. for Ontario.

---

## 7. REFERENCES

- [1] D. Nicolaides, D. Cebon, and J. Miles, "An urban charging infrastructure for electric road freight operations: A case study for Cambridge UK," *IEEE Syst. J.*, vol. 13, no. 2, pp. 2057–2068, Jun. 2019.
- [2] M. Mohamed, H. Farag, N. El-Taweel, and M. Ferguson, "Simulation of electric buses on a full transit network: Operational feasibility and grid impact analysis," *Electr. Power Syst. Res.*, vol. 142, pp. 163–175, Jan. 2017.
- [3] N. A. El-Taweel, H. E. Z. Farag and M. Mohamed, "Integrated Utility-Transit Model for Optimal Configuration of Battery Electric Bus Systems," in *IEEE Systems Journal*, 2020.
- [4] M. Mahmoud, R. Garnett, M. Ferguson, and P. Kanaroglou, "Electric buses: A review of alternative powertrains," *Renew. Sustain. Energy Rev.*, vol. 62, pp. 673–684, Sep. 2016.
- [5] P. Bonami et al., "An algorithmic framework for convex mixed integer nonlinear programs," *Discrete Optim.*, vol. 5, no. 2, pp. 186–204, May 2008.
- [6] P. Bonami and J. P. M. Gonçalves, "Heuristics for convex mixed integer nonlinear programs," *Comput. Optim. Appl.*, vol. 51, no. 2, pp. 729–747, Mar. 2012
- OPTI Toolbox, "Basic Open Source Nonlinear Mixed Integer Programming." [Online]. Available: <https://www.inverseproblem.co.nz/OPTI/index.php/Solvers/BONMIN>
- [7] M.V. Kirthiga, S. A. Daniel, and S. Gurunathan, "A methodology for transforming an existing distribution network into a sustainable autonomous micro-grid," *IEEE Trans. Sustain. Energy*, vol. 4, no. 1, pp. 31–41, Jan. 2013.
- [8] American National Standard for Electric Power Systems and Equipment–Voltage Ratings (60 Hertz), ANSI Std. C84.1, Dec. 2006.
- [9] N. A. El-Taweel and H. E. Z. Farag, "Incorporation of Battery Electric Buses in the Operation of Intercity Bus Services," *2019 IEEE Transportation Electrification Conference and Expo (ITEC)*, Detroit, MI, USA, 2019, pp. 1-6.
- [10] M. Smith and J. Castellano, "Costs associated with non-residential electric vehicle supply equipment: Factors to consider in the implementation of electric vehicle charging stations," US Department of Energy, Washington, DC, USA, Rep. DOE/EE-1289, Nov. 2015.
- [11] S. Chung and O. Trescases, "Hybrid energy storage system with active power–mix control in a dual–chemistry battery pack for light electric vehicles," *IEEE Trans. Transp. Electr.*, vol. 3, no. 3, pp. 600–617, Sep. 2017.
- [12] N. A. El-Taweel, M. Mohamed, and H. E. Farag, (2017), "Optimal design of charging stations for electrified transit networks," in *2017 IEEE Transportation Electrification Conference and Expo (ITEC)*, pp. 786–791, 2017.
- ABB (2018), "Opportunity charging for electric buses".
- [13] L. Eudy, M. B. Post, Fuel cell buses in us transit fleets: Current status 2017, Technical Report, National Renewable Energy Lab (NREL), Golden, CO (United States), 2017.
- Available at: <http://new.abb.com/ev-charging/products/opportunity-charging> (Accessed on February 2020).
- [14] G. De Filippo, V. Marano, and R. Sioshansi (2014), "Simulation of an electric transportation system at The Ohio State University," *Appl. Energy*, vol.113, pp. 1686–1691, Jan. 2014.
- [15] A. Lajunen, T. Lipman, Lifecycle cost assessment and carbon dioxide emissions of diesel, natural gas, hybrid electric, fuel cell hybrid and electric transit buses, *Energy* 106 (2016)329–342.